# VALIDATION OF CASPASE-INDEPENDENT CELL DEATH INDUCING PROPERTIES OF GERANYLATED 4-PHENYLCOUMARINS ISOLATED FROM *Mesua elegans* ON PROSTATE CANCER CELL LINES

HANI BINTI SAPILI

FACULTY OF SCIENCE
UNIVERSITY OF MALAYA
KUALA LUMPUR

2019

# VALIDATION OF CASPASE-INDEPENDENT CELL DEATH INDUCING PROPERTIES OF GERANYLATED 4-PHENYLCOUMARINS ISOLATED FROM *Mesua elegans* ON PROSTATE CANCER CELL LINES

**HANI BINTI SAPILI**

**THESIS SUBMITTED IN FULFILMENT OF THE REQUIREMENTS FOR THE DEGREE OF MASTER OF SCIENCE**

**INSTITUTE OF BIOLOGICAL SCIENCES**
**FACULTY OF SCIENCE**
**UNIVERSITY OF MALAYA**
**KUALA LUMPUR**

**2019**

**UNIVERSITY OF MALAYA**

**ORIGINAL LITERARY WORK DECLARATION**

Name of Candidate: **HANI BINTI SAPILI**

Matric No: **SGR150016**

Name of Degree: **MASTER OF SCIENCE**

Title of Project Paper/Research Report/Dissertation/Thesis ("this Work"):

**VALIDATION OF CASPASE-INDEPENDENT CELL DEATH INDUCING PROPERTIES OF GERANYLATED 4-PHENYLCOUMARINS ISOLATED FROM *Mesua elegans* ON PROSTATE CANCER CELL LINES**

Field of Study: **GENETICS AND MOLECULAR BIOLOGY**

I do solemnly and sincerely declare that:

(1) I am the sole author/writer of this Work;
(2) This Work is original;
(3) Any use of any work in which copyright exists was done by way of fair dealing and for permitted purposes and any excerpt or extract from, or reference to or reproduction of any copyright work has been disclosed expressly and sufficiently and the title of the Work and its authorship have been acknowledged in this Work;
(4) I do not have any actual knowledge nor do I ought reasonably to know that the making of this work constitutes an infringement of any copyright work;
(5) I hereby assign all and every rights in the copyright to this Work to the University of Malaya ("UM"), who henceforth shall be owner of the copyright in this Work and that any reproduction or use in any form or by any means whatsoever is prohibited without the written consent of UM having been first had and obtained;
(6) I am fully aware that if in the course of making this Work I have infringed any copyright whether intentionally or otherwise, I may be subject to legal action or any other action as may be determined by UM.

Candidate's Signature Date:

Subscribed and solemnly declared before,

Witness's Signature Date:

Name:

Designation:

**VALIDATION OF CASPASE-INDEPENDENT CELL DEATH INDUCING PROPERTIES OF GERANYLATED 4-PHENYLCOUMARINS ISOLATED FROM *Mesua elegans* ON PROSTATE CANCER CELL LINES**

## ABSTRACT

Geranylated 4-phenylcoumarins DMDP-1 and DMDP-2 isolated from *Mesua elegans* were elucidated for their role in inducing caspase-independent programmed cell death (CI-PCD) in prostate cancer cell lines, PC-3 and DU 145, respectively. The half maximal inhibition concentration value ($IC_{50}$) identified through MTT assay of DMDP-1 is 13μM for PC-3 cells, while DMDP-2 is 9μM for DU 145 cells. Cell homeostasis disruption was demonstrated upon treatment, as shown by the increase in calcium ion through colourimetric assay and endoplasmic reticulum (ER) stress markers GRP 78 and p-eIF2α through western blot. Subsequently, cytoplasmic death protease calpain-2 also showed increased activity during DMDP-1 & -2 treatments, while lysosomic death protease cathepsin B activity was significantly increased in PC-3 treated with DMDP-1. Flow cytometry showed a reduction in mitochondrial membrane potential in both cell lines, while western blotting showed translocation of mitochondrial death protease AIF into the cytoplasm in its truncated form. Furthermore, DMDP-1 & -2 treatments caused significant increase in superoxide level and oxidative DNA damage. Concurrent inhibition of calpain-2 and cathepsin B during the treatment showed an attenuation of cell death in both cell lines. Hence, DMDP-1 & -2 induce CI-PCD in prostate cancer cell lines through calpain-2 and cathepsin B.

**Keywords:** coumarins, prostate cancer, caspase-independent cell death

**PENGENALPASTIAN MEKANISME KEMATIAN SEL DIPROGRAMKAN TANPA KASPASE OLEH GERANYLATED 4-PHENYLCOUMARINS YANG DIEKTSRAK DARIPADA *Mesua elegans* PADA SEL KANSER PROSTAT**

## ABSTRAK

Geranylated 4-phenylcoumarins DMDP-1 dan DMDP-2 yang diasingkan daripada *Mesua elegans* telah dianalisa untuk mengenal pasti peranan mereka dalam mengakibatkan kematian sel diprogramkan tanpa kaspase (CI-PCD) pada dua sel kanser prostat, PC-3 dan DU 145. Eksperimen MTT menunjukkan nilai $IC_{50}$ DMDP-1 bagi PC-3 adalah 13μM dan DMDP-2 bagi DU 145 adalah 5μM. Gangguan pada homeostasis sel juga terbukti semasa rawatan, seperti mana yang ditunjukkan dalam peningkatan ion kalsium melalui ujian pewarnaan dan penanda stres endoplasmik retikulum (ER)- GRP 78 dan p-eIF2α yang dinilai melalui pemblotan western. Selanjutnya, protein kalpain-2 juga menunjukkan peningkatan aktiviti semasa rawatan DMDP-1 & -2, sementara aktiviti protein katepsin B meningkat dengan ketara dalam PC-3 yang dirawat dengan DMDP-1. Eksperimen flow sitometri menunjukkan penurunan ketara pada nilai potensi membran mitokondria, manakala eksperimen pemblotan westen menunjukkan translokasi protein AIF yang terletak di mitokondria ke sitoplasma. Rawatan DMDP-1 & -2 juga mampu menunjukkan peningkatan ketara pada tahap superoksida dan kerosakan DNA disebabkan oleh stres oksidatif. Perencatan aktiviti kedua-dua protein kalpain-2 dan katepsin B semasa rawatan menunjukkan kematian sel tergendala pada kedua-dua jenis sel prostat. Kesimpulannya, DMDP-1 & -2 menyebabkan CI-PCD dalam sel-sel kanser prostat melalui pengaktifan kalpain-2 dan katepsin B.

**Keywords:** coumarins, kanser prostat, kematian sel diprogramkan tanpa kaspase

## ACKNOWLEDGEMENTS

With the name Allah, the most gracious and most merciful, all praise to him for everything that he has bestowed me with. This work would not have been possible without the guidance, help and support from various individuals and parties throughout this study. The sincerest thank and acknowledgement to my dear supervisor Prof. Dr. Noor Hasima Nagoor who has not only guided, supervised me, but has always been patient with me. As my teacher and mentor, she has extensively supported me professionally and personally more than I could ever give her credits for here. Next, I would like to thank University of Malaya and Ministry of Higher Education for the funding channeled in this study. I am thankful to every each of the members of the Cancer Research Lab for their supports and advices, especially to Dr. Sharan Malagobadan for his close guidance and help throughout my study and in the process of this writing. Not to forget, Dr. Dennise Ho and Dr. Norhafiza Arshad for their experimental and technical guidance.

Being away from home in this journey, I would like to acknowledge those people who have always been around through my ups and downs, my dearest friends Herlveron, Amirul, Ainil, Abdullah, Abu and Chris. Nobody has been more important to me in the pursuit of this project than the members of my family. I would like to thank my parents and my siblings; whose love and supports are with me in whatever I pursue. A special dedication to my late mother, who had passed away during the final year of this study, my eternal love and appreciation for her, who has always been my strength and inspiration. Thank you for all the supports, there is no word can describe how grateful I am for everything she had done for me, especially during this study. She had fought well in her battle with breast cancer, it's time for her to rest, may she rest in peace.

## TABLE OF CONTENTS

## LIST OF FIGURES

## LIST OF TABLES

## LIST OF SYMBOLS AND ABBREVIATIONS

| | | |
|---|---|---|
| α | : | Alpha |
| °C | : | Degree celcius |
| μg | : | Microgram |
| (IRE)1α | : | Inositol requiring enzyme |
| μL | : | Microliter |
| μm | : | Micrometer |
| μM | : | Micromolar |
| AIF | : | Apoptotic inducing factor |
| ATF | : | Activating transcription factor |
| ATP | : | Adenosine triphosphate |
| CA-074 | : | (L-3-trans-(Propylcarbamyl)oxirane-2-carbonyl)-L-isoleucyl-L-proline |
| CD-PCD | : | Caspase dependent-programmed cell death |
| CI-PCD | : | Caspase independent-programmed cell death |
| $CO_2$ | : | Carbon dioxide |
| dL | : | Deciliter |
| DMDP-1 | : | (5, 7-dihydroxy-8-(2-12methylbutanoyl)-6-[(E)-3, 7-dimethylocta-2,6-dienyl]-4-phenyl-2H-chromen-2-one |
| DMDP-2 | : | (5, 7-dihydroxy-8-(3-methylbutanoyl)-6-[(E)-3, 7-dimethylocta-2,6-dienyl]-4-phenyl-2H-chromen-2-one |
| DU 145 | : | Duke University 145 |
| DNA | : | Deoxyribonucleic acid |
| EDTA | : | Ethylenediaminetetraacetic acid |
| ER | : | Endoplasmic reticulum |

| | | |
|---|---|---|
| FBS | : | Fetal bovine serum |
| GRP78 | : | Glucose regulating protein 78 |
| $H_2O$ | : | Water |
| $IC_{50}$ | : | half maximal inhibitory concentration |
| IUCN | : | International Union for Conservation of Nature |
| kbp | : | Kilo base pairs |
| kDa | : | Kilo Dalton |
| mg | : | Milligram |
| MIM | : | Mitochondrial inner membrane |
| MOMP | : | Mitochondrial outer membrane permeabilization |
| MPT | : | Mitochondrial permeability transition |
| MTT | : | 3-(4,5-dimethylthiazol-2-yl)-2,5-diphenyltetrazolium bromide |
| NADH | : | Nicotinamide adenine dinucleotide |
| nm | : | Nanometer |
| NSCLC | : | Non-small-lung carcinoma |
| $O_2^-$ | : | Superoxide |
| OD | : | Optical density |
| p-eif2 | : | Phosphorylated-eukaryotic initiation factor alpha |
| PBS | : | Phosphate buffered saline |
| PCD | : | Programmed cell death |
| PERK | : | PKR-like eukaryotic initiation factor (eIF)2α kinase |
| PC-3 | : | Prostate cancer 3 |
| REAP | : | Rapid efficient and practical |
| ROS | : | Reactive oxygen species |
| RPMI | : | Roswell Park Memorial Institute |
| S.D | : | Standard deviation |

| | | |
|---|---|---|
| UPR | : | Unfolded protein response |
| WHO | : | World's Health Organization |

## LIST OF APPENDICES

# CHAPTER 1: INTRODUCTION

Isolation of natural compound for cancer prevention and treatment is well established in cancer research and therapy (Nobili et al., 2009). In this study, geranylated 4-phenylcoumarins (DMDP) isolated from a plant called *Mesua elegans* were investigated for its potentials to induce programmed cell death (PCD) in prostate cancer cells. DMDP existed in analogues, DMDP-1 and DMDP-2 due to the isomerism at the attached methyl butanoyl group. In previous study, DMDP-1 & -2 were proven to have high toxicity effects on two prostate cancer cell lines PC-3 and DU 145 respectively by inducing caspase-independent programmed cell death (CI-PCD) (Suparji et al., 2016). One of the important factors in a drug study is measurement of the half maximal inhibitory concentration, the $IC_{50}$ value (Caldwell et al., 2012), where a lower $IC_{50}$ value signifies higher potency of the compound on the cancer cells. $IC_{50}$ values of DMDP-1 & -2 were measured through MTT assay and determined to be 13μM for DMDP-1 in PC-3 and 5μM in DU 145 cell lines.

Disruption of cellular homeostasis is an important parameter of cell death that among many can be indicated by the intracellular $Ca^{2+}$ elevation and increase in endoplasmic reticulum (ER) stress. (Kreb et al., 2015). PC-3 and DU 145 cells treated with their respective analogues have proven to elevate intracellular $Ca^{2+}$ and ER stress. Studies done in the past decade have shown that in the absence of caspases activation, PCD can be mediated by other death proteins (Constantinou et al., 2009). DMDP-1 & -2 were shown to activate calpain-2 in PC-3 and DU 145 cells and cathepsin B in DMDP-1 treated PC-3 cells. Interestingly, inhibition of calpain-2 and cathepsin B with their respective inhibitors concurrently were able to attenuate cell death.

Another death related protein located in the mitochondria, apoptotic inducing factor (AIF) was released into the cytoplasm upon treatment with the analogues while flow

cytometry analysis showed a reduction in the mitochondrial membrane potential ($\Delta\psi M$) in the cells. AIF exhibits NADH oxidase activity to form the superoxide ($O_2^-$). The superoxide formation measured with flow cytometry was significantly increased in the analogs treated cells.

The final hallmark of cell death is the induction of DNA damage (Surova & Zhivotosky, 2013). In this study, DNA damage by oxidative stress was detected in the cells upon treatment.

In conclusion, this study investigated the mechanisms of CI-PCD induced by DMDP-1 & -2 in both PC-3 and DU 145 cell lines respectively as a potential therapeutic target for prostate cancers.

### 1.1 Problem statement

Prostate cancer is one of the most common cancers as well as the second leading cause of cancer related deaths in men. Despite the availability of multiple treatment options including surgery, radiation therapy, chemotherapy or hormonal therapy, there are currently no effective therapies available for the treatment of androgen-independent prostate cancer, which often arises after hormonal deprivation or ablation therapy. Therefore, it is important to find alternative effective treatment for this particular type of prostate cancer.

Also, resistance to apoptosis has become a serious problem to the treatment of cancer. A compound that can induce death through multiple mechanisms would be ideal to address the issue.

Previous study with the DMDP-1 & -2 has shown significant caspase-independent cytotoxicity. A protein array and western blot analysis suggested the involvement of more

than one death organelles, the lysosome and endoplasmic reticulum but not the mitochondria.

Therefore, this project aims to validate and provide a better understanding of the death mechanisms that are involved and the mode of action of these compounds in its application to treat cancer cells which are apoptosis resistance.

## 1.2 Hypothesis

DMDP-1 & -2 sensitize prostate cancer cells by triggering caspase-independent cell death involving activation of death factors, namely cathepsin B and calpain 2 leading to lysosomal and endoplasmic reticulum cell death respectively.

## 1.3 Objectives

Therefore, the objectives of the study are:

*i* To investigate the mechanism of death induced in two prostate cancer cell lines – PC-3 and DU 145 after treatment with two geranylated 4-phenylcoumarins – DMDP-1 and DMDP-2 respectively.

*ii* To investigate death proteases involved in the cell death induced by geranylated 4-phenylcoumarins DMDP-1 & DMDP-2 in PC-3 and DU 145 respectively.

*iii* To assess the suitability of these compounds as potential cancer therapeutic agents.

# CHAPTER 2: LITERATURE REVIEW

## 2.1 Cancer

The term cancer originated from the Greek word for crab, *karkinoma*, which was later called cancer in Latin. It was first used in a description of cancer by Hippocrates 2,300 years ago in his observation, based on the formation of swollen veins on a breast tumour that resembled a crab's leg (Lakhtakia, 2014). Cancer can result from accumulated disruptions in cellular regulatory systems causing abnormal cell proliferation and invasion to surrounding normal tissues and throughout the body. It is a multistep process that increases the cell's capacity for proliferation, survival and invasion. The first step is the tumour initiation when genetic alteration causes abnormal proliferation of the cell to form a colony termed as tumour. Next is the tumour progression, when additional mutations in the cell colony grant selective advantages to override normal regulatory systems, such as growth, differentiation, migration and survival. Through clonal selection, cells within the colony that exhibit these mutated properties will become dominant and continue to grow rapidly and become increasingly malignant (Cooper, 2000)

### 2.1.1 Prostate cancer

Cancer is the second leading cause of death in human worldwide based on the most recent data in 2018 by World Health Organization (WHO), with approximately 9.6 million cancer related death reported (WHO, 2018). This indicates that one out of six deaths reported globally is due to cancer. Prostate cancer has remained one of the major cancers and is the second most common cancer in men, after lung cancer (Bray et al., 2018). In Malaysia, it is the 6$^{th}$ top cancer in men and accounts for 8.8% of cancer diagnosis in 2018, an increase from 5.7% in 2014 (Bray et al., 2018). The number of prostate cancer cases is predicted to grow higher in the future year due to considerably

low awareness among Malaysian towards the importance of early diagnosis of prostate cancer and healthy lifestyle (Sothilingam et al., 2010).

Prostate cancer is classified as adenocarcinoma due to the fact it is initiated in the glands of the peripheral zone and continue to grow in glandular structure. The thickening of the epithelial layer and loss of distinct basal and secretory layers is known as prostatic intraepithelial neoplasia (Biagioli et al., 2008), which is the earliest precursor histologically detected. Prostate cancers are frequently observed to be multifoci, where distinct carcinoma and PIN in varying degree of dysplasia, tissue disorganisation and genetic alteration can be found within one prostate (Schulz et al., 2003).

Though the rate of cell proliferation in prostate cancer is low, the abnormal increase of cell number is mainly due to the inappropriately low rate of apoptosis. Several mutations in apoptotic genes are known to contribute to prostate cancer development and formation. For example, overexpression of anti-apoptotic protein Bcl-2 is found in approximately half of all prostate cancers, particularly in androgen-independent cases (McDonnell et al., 1992). Additionally, increased expression of several growth factor receptors, such as tyrosine kinase receptors EGFR or ET1A receptor for endothelins, may increase the responsiveness of prostate cancer cells to endothelin and local paracrine signalling during the occurrence of bone metastasis (Nelson & Carducci, 2000; Schulz et al., 2003).

### 2.1.2 Prostate cancer cell lines

There are several cell lines derived from prostate cancer patients used in the biological field to better understand the mechanism of the cancer and treatment strategy. PC-3 and DU 145 are among the most commonly used prostate cancer cell lines in cancer research.

#### 2.1.2.1 PC-3

PC-3 is an androgen independent ATCC prostate cancer cell line derived from a 62-year old Caucasian male. The metastasis site of the cell line is the lumbar region of the bones. It is also found to exhibit a deletion mutation of the p53 gene.

#### 2.1.2.2 DU 145

DU 145 is another cell line commonly used for prostate cancer study. This cell line is androgen independent and was derived from a 69-year old Caucasian male from the central nervous system metastatic site. It has a p53 mutation at codons 223 and 274. The cell line also shows a mutation in p16, a cell cycle control gene.

## 2.2 Natural compound

### 2.2.1 *Mesua elegans*

*Mesua elegans* is categorized under the Clusiacease family which formerly known as Guttifire. Plants from the family are consists of 40 genera and more than 1000 species and mainly distributed in the tropical regions with the least abundance in Africa. There are four genera of the Clusiacease family in the Peninsular Malaysia which includes *Calophyllum, Garcinia, Mammea and Mesua* (Gomathi, 2015)

Colloquially, *Mesua elegans* is known as 'pokok penaga'. It is widely distributed in the lowlands and sub-montane forests, its estimated numbers classify it as a low-risk endangered species by the IUCN (Kochummen, 1998).

**Table 2.1: *Mesua elegans* taxonomy**

| | |
|---|---|
| Kingdom: | Plantae |
| Phylum: | Tracheophyta |
| Class: | Magnoliopsida |
| Order: | Theales |
| Family: | Clusiacease (Guttifire) |
| Scientific Name: | *Mesua elegans* |

**Figure 1.1: The inner bark and flower of *Mesua elegans***

Plant from the genus *Mesua* are bushes or small to large trees. *Mesua elegan* is considered medium in the *Mesua* genus in which it can reach a height up to 8 meter and 15cm in diameter. The leaves were thinly coriaceous, it has short petioles and its flowers are white. The bark is described to be scaly, greyish brown in colour with pinkish brown inner bark (Gomathi, 2015).

Compounds extracted from *Mesua elegans* were reported to have an anti-acetylcholinesterase (AChE)- key enzyme in the cholinergic nervous system. In which inhibition of the protease improves cholinergic functions in patients with Alzheimer's

disease and alleviates the symptoms of the disorder (Garcia et al., 2011; Murray et al., 2013).

However, no traditional application of the *Mesua elegan* has been recorded to this point unlike the other genus from the *Mesua* family *Mesua ferrea* which was the most widely studied plant in the genus. *Mesua ferrea* has been reported to be used as anti-septic, anti-asthmatic and anti-allergic traditionally (Gomathi, 2015).

### 2.2.2 Coumarins

Coumarins are metabolic products of the amino acids phenylalanine and tyrosine through the phenylpropanoid pathway. There are many variations of coumarin found in nature, and different plants produce different repertoires of these secondary metabolites. They are synthesised through hydroxylation, glycolysis and cyclization of cinnamic acid into the intermediary molecule benzo-α-pyrone, which is further modified into the final compound (Tosun, 2012).

Coumarins have been reported to not only have biologically important defensive functions within their plants of origin but also significantly useful to combat cancer, microbial infections, allergies and oxidative stress in humans (Hoult & Paya, 1996). It is particularly notable for its hepato-protective effects in inhibiting the activity of several liver enzymes (Hoult & Paya, 1996; Kostova, 2006). However, many natural coumarins are unsuitable for therapeutic usage as they exhibit toxic and carcinogenic properties. As such, use of modified coumarins, either through synthetic addition of side chains or by extraction of a coumarin derivatives, has shown to be safer and more effective against cancer (Kostova, 2006). For example, 4-phenylcoumarins are products of further processing of coumarins, and it forms the backbone of neoflavones, a medicinally important plant-based substance. Meanwhile, geranylated phenylcoumarins isolated from

*Mammea siamensis* flower have exhibited apoptotic-pathway inducing effects on cancer cell lines without cytotoxicity on normal epithelial cell lines (Tung et al., 2013).

### 2.2.3 DMDP-1 and DMDP-2

DMDP-1 ((5, 7-dihydroxy-8-(2-12methylbutanoyl)-6-[(E)-3, 7-dimethylocta-2,6-dienyl]-4-phenyl-2H-chromen-2-one) and DMDP-2 ((5, 7-dihydroxy-8-(3-methylbutanoyl)-6-[(E)-3, 7-dimethylocta-2,6-dienyl]-4-phenyl-2H-chromen-2-one) are two types of geranylated 4-phenylcoumarins extracted from the hexane extract of *Mesua elegans* bark. These compounds have been tested for their anti-cancer properties and the pathways mediated in a preliminary study (Suparji et al., 2016).

## 2.3 Programmed cell death

Programmed cell death (PCD) is a highly regulated process of cell death that is crucial in the development and homeostasis of living organisms (Ameisen, 2002). One of the most desired PCD, apoptosis, was originally characterised by its change in morphology during the process of cell death (Kerr et al.,1972). In the cell nucleus, DNA will be fragmented, and chromatin condensation will occur. Detachment of cells from their actin cortex will lead to the protrusion of the plasma membrane to form bleb. When cells shrink, the bleb will be released to form apoptotic body packed with organelles and nuclear fragments that will be engulfed by neighbouring phagocytes (Charras, 2008; Ziegler & Groscurth, 2004).

### 2.3.1 Disruption in cellular homeostasis

Cell survival is dictated by its system's efficiency in regulating balance in the cell. Typically, exposure of cells to any death stimuli initiates a cell death pathway which will disrupt cellular homeostasis (Rager, 2015).

#### 2.3.1.1 Intracellular $Ca^{2+}$ level

$Ca^{2+}$ is critically involved in cellular signalling and a change of its function will lead to disruptions in the cell. $Ca^{2+}$ is found to be abundant in endoplasmic reticulum (ER) and mitochondria, the organelles which act as a $Ca^{2+}$ reservoirs. The low level of $Ca^{2+}$ in the cytosol enables it to act as a regulator for cytosolic $Ca^{2+}$ dependent enzymes. As such, maintenance of $Ca^{2+}$ homeostasis, with a low and stable concentration of $Ca^{2+}$ in the cytosol, is required for efficient $Ca^{2+}$ signalling. One of the mechanisms commonly used in $Ca^{2+}$ regulation is the active pumping against its gradient by $Ca^{2+}$ATPases. $Ca^{2+}$ATPases are present on the cytosolic side of plasma membrane and endoplasmic reticulum (ER) to perform high energy task of pumping $Ca^{2+}$ out of the cytosol against the gradient. This can also be mediated by ion exchangers (Cerella et al., 2010).

$Ca^{2+}$ signalling requires strict cooperation among different cellular compartments and organelles, especially between the ER and mitochondria. These two organelles contain $Ca^{2+}$ - mediating transport system that interacts through highly dynamic physical connections to control exchange of $Ca^{2+}$ essential for cellular functions (Brand et al., 2013; Cerella et al., 2010).

However, excess or deregulated cellular $Ca^{2+}$ concentration can result in cellular toxicity. Pathological $Ca^{2+}$ alteration will result in failure of homeostatic controls while loss in $Ca^{2+}$ balance will lead to apoptosis or necrotic cell death, depending on the intensity of the damage inflicted (Cerella et al., 2010).

#### 2.3.1.2 Endoplasmic reticulum (ER) Stress

The ER is essential in multiple cellular processes required for cell survival and normal cellular functions, such as intracellular calcium homeostasis, protein secretion and lipid biosynthesis. As such, ER acts an efficient sensor for cellular stress. ER stress occurs in

response to various stimuli of physiological and pathological conditions that lead to accumulation of unfolded and misfolded proteins in the ER. As a consequent, unfolded protein response (UPR) is triggered to resolve the stress through activation of intracellular signal transduction pathways (Bravo-Sagua et al., 2013).

Under basal condition, a chaperone protein GRP78/Bip inhibits three ER membrane-associated proteins UPR mediators, namely, inositol requiring enzyme (IRE)1α, PKR-like eukaryotic initiation factor (eIF)2α kinase (PERK) and activating transcription factor (ATF). Upon ER stress, the three proteins will be activated when released from GRP78. These proteins are responsible for the alleviation of accumulated misfolded proteins in the ER by enhancing the protein folding capacity. This can either be by inhibiting new protein synthesis or speeding degradation of misfolded proteins. However, if the ER function is not restored or the extensive ER stress is not stopped, cell death will eventually be induced through activation of apoptosis (Bravo-Sagua et al., 2013).

### 2.3.2 Caspase-dependent Programmed Cell Death

PCD is classically known to be mediated by the caspase enzyme family. Caspases have proteolytic activity and are able to cleave proteins at aspartic acid residues, although different caspases have different specificities involving recognition of neighbouring amino acids (Elmore, 2007). Accordingly, caspases have been broadly classified by their known roles in apoptosis in mammals, which are caspase-3, -6, -7, -8, and -9. These caspases can be further sub-classified based on their mechanism in PCD, as either initiator caspases (caspase-8 and -9) or executioner caspases (caspase-3, -6, and -7) (McIlwain et al., 2013). Caspases activation irreversibly commits cells towards cell death through initiation of proteolytic cascades (Elmore, 2007). There are two pathways in the caspase-dependent PCD (CD-PCD), which are the extrinsic (receptor mediated) and the intrinsic pathways (mitochondrial mediated).

#### 2.3.2.1 Extrinsic pathway

In the extrinsic pathway, the binding of protein ligands to the cell surface receptors such as tumour necrosis factor receptor 1 (TNFR1), cluster of differentiation 95 (CD95) and TNF related apoptosis inducing ligands (TRAIL) will result in their oligomerization and formation of death inducing signalling complex (DISC), activation of caspase-8 and downstream executioner caspase-3 (Zhivotovsky & Orrenius, 2010b).

#### 2.3.2.2 Intrinsic pathway

In the intrinsic pathway, non-receptor mediated stimuli work in a positive or negative fashion to trigger the activation of PCD (Elmore, 2007). Direct activation of caspase-3 or cleavage of BH3 interacting domain death agonist (BID) will result in mitochondrial dysfunction and subsequent release of cytochrome c into the cytosol to induce cell death (Loreto et al., 2014).

### 2.3.3 Caspase-independent programmed cell death

Around the year of 1997, reports have emerged showing that PCD can still take place without the activation of caspases (Hirsch et al., 1997; Ohta et al., 1997; Sarin et al., 1997; Tait & Green, 2008). In these reports, inhibition of caspases activity was unable to attenuate cell death in cells exposed to death stimuli. This kind of cell death is categorised as caspase-independent programmed cell death (CI-PCD) (Broker et al., 2005; Tait & Green, 2008; Constantinou et al., 2009). This discovery had opened a new focus worth exploring in cell death study, which holds a promising potential in understanding cellular pathology and disease therapy including cancer (Tait & Green, 2008; Fitzwalter & Thorburn, 2015).

Since its discovery, there have been a plethora of studies reported on CI-PCD to better understand its underlying mechanism. Some of the major findings of such studies centred

around the role of multiple organelles and proteases mediating cell death (Constantinou et al., 2009).

#### 2.3.3.1 Endoplasmic reticulum pathway

The endoplasmic reticulum (ER) is a versatile organelle which carries out multiple functions in the cell, such as calcium transport and protein folding, amongst others. ER stress induced cell death (ERCD) is triggered primarily by the accumulation of proteins within the organelle or the excessive release of calcium ions (Sano & Reed, 2013). Typically, these events culminate in mitochondria disruption and the activation of apoptotic factors such as caspases and calpains (Smith & Schnellmann, 2012).

(a) **Calpains**

Intracellular calcium release often results in the activation of calpains, a family of cysteine proteases that require calcium ion ($Ca^{2+}$) for activation. Calpains are known to possess various roles in calcium-regulated cellular processes such as signal transduction, cell proliferation, cell cycle progression, differentiation, apoptosis, membrane fusion and platelet activation. As such, impairment of its function has been reported in variety of pathological conditions such as Alzheimer's disease, cancer metastasis, cataract formation and neuronal degeneration (Ono et al., 2004).

There are two conventional species of calpain family in mammals, which are the μ-calpain and m-calpain or calpain-1 and calpain-2, respectively. The activation of these two calpains depends on the level of the intracellular calcium. Calpain-1 is sensitive to micromolar (μM) level of intracellular $Ca^{2+}$, while calpain-2 is sensitive towards millimolar (mM) level. They are both heterodimers consisting of an 80kDa and a 30kDa regulatory subunits. The 80kDa subunit is composed of 4 domains (I-IV) while the 30kDa subunit consists of two (V-VI). Both domains IV and VI contain five sets of EF-hand $Ca^{2+}$ binding motifs.

In the presence of $Ca^{2+}$, calpain-1 and -2 dissociate into their respective subunits, where the dissociated 80kDA subunit functions as an active species *in vivo*. Studies on the calpain-2 activity elucidated that it exists in the cytosol as an inactive enzyme. In response to the increase of intracellular $Ca^{2+}$, calpain-2 will translocate to the cell membrane before being activated upon binding with $Ca^{2+}$. Then, autocatalytic hydrolysis of domain I takes place and the 30kDa subunit will dissociate from the 80K subunit. The activated 80kDA hydrolyses the subunits in the membranes or cytosol (Ono et al., 2004).

Calpain-2 has been reported to regulate the activity of effector caspases such as caspase-7 and caspase-8 and affect expression of the Bcl-2 family members, which in turn leads to mitochondrial outer membrane permeabilization (MOMP). However, calpain-2 has also exhibited the ability to induce apoptosis-like cell death without the involvement of caspases. This happens particularly during platelet activation and excitotoxic neuron death (Volbracht et al., 2005; Lopatniuk & Witkowski, 2011), during which the activated calpains produce apoptosis-like characteristics within the affected cells, such as phosphatidylserine exposure, chromatin condensation and cell shrinkage.

#### 2.3.3.2 Lysosomal pathway

In the past, lysosomes were only regarded as an aid in the necrotic and apoptotic processes. Within the cell, they serve the function of a recycling centre and contain many hydrolases which could digest macromolecules during the cell degradation process. It is now known that lysosomal membrane permeabilization (LMP) can lead to cell death via lysosome pathway (Boya & Kroemer, 2008; Repnik et al., 2014). However, LMP is not an exclusive characteristic of lysosomal cell death (LCD) and can be seen in the later stages of necrosis and other PCDs. Therefore, LMP can both initiate and amplify cell death (Repniket al., 2013).

Presently, methods that are sophisticated enough to distinguish whether an LMP event is the instigative factor of cell death or is a response to upstream elements are unavailable. *In vivo* LMP and subsequent LCD can be induced by viral proteins, bacterial toxins, reactive oxygen species (ROS), lyso-osmotropic detergents and TNF administration (Boya & Kroemer, 2008).

(a) **Cathepsins**

Although cathepsins are conventionally known to be localised in the lysosomes, they are able to permeabilise into the cytosol. There are 2 serine and 11 cysteine cathepsins, based on the proteolysis site of the enzyme. All cathepsins require a reducing acidic environment to be optimally active, which explains the necessity of the localisation in the lysosomes. Cathepsins B and D in particular are stable proteins and play important roles in apoptotic and necrotic-like PCD (Qi & Liu, 2006).

Cathepsin B is known to play a role in the processing of Bid and caspase-2. It also has roles in the production of reactive oxygen species (ROS) and degradation of Bcl-2, Bcl-xL and Bak. These events lead to the mitochondrial membrane permeabilization and cytochrome c release.

Recently, cathepsin B has also been reported to be involved in the induction of cell death in absence of caspases activation by activating other proteases such as calpain-2 or apoptotic inducing factor (AIF) or inducing ROS formation. For the purpose of pathway identification, cathepsin B is perhaps the protein representing the LCD pathway more definitively. Meanwhile, the other family of cathepsin B, cathepsin D has the ability to activate Bid and trigger Bax-mediated cytochrome c release. Therefore, cathepsin D has been widely implicated in MOMP, leading to the apoptosis intrinsic pathway, whereas cathepsin B is more likely to cause LCD independent of the caspase-dependent apoptotic machinery (Appelqvist et al., 2012).

#### 2.3.3.3 Mitochondrial pathway

Several intracellular signals, including DNA damage and endoplasmic reticulum (ER) stress, converge on the mitochondrial pathway to induce mitochondrial membrane permeabilization (MMP) to provide the decision for survival or death.

To understand the mechanisms of MMP, it is important to determine the permeabilization events affecting the mitochondrial inner membrane (MIM) or mitochondrial outer membrane (MOM). MOM is normally permeable to metabolites but not to proteins, meaning that MOM permeabilization is mostly assessed by determining the translocation of proteins through MOM, from the inter-membrane space to the extra-mitochondrial compartment. In contrast, MIM is usually impermeable to ions and water, so its permeabilization is measured by physicochemical methods assessing the capacity of MIM to maintain an electrochemical gradient or to separate low molecular weight solutes from each other.

Intrinsic or mitochondrial pathway of apoptosis involve stimuli that cause changes in the inner mitochondrial membrane (MIM), which results in an opening of the mitochondrial permeability transition pore, loss of the mitochondrial transmembrane potential and release of sequestered pro-apoptotic proteins from the intermembrane space into the cytosol (Elmore, 2007; Kourtis & Tavernarakis, 2009). The stimuli that initiate the intrinsic pathway produce intracellular signal that may act in either a positive fashion, such as responses towards radiation, toxins, hypoxia, hyperthermia, viral infection and free radicals or negative fashion, such as responses seen in the absence of growth factors, hormones and cytokines (Tait & Green, 2008; Fitzwalter & Thorburn, 2015).

In healthy cells, the mitochondrial inner membrane is normally restricted to all ions, including protons. This will generate a proton gradient that is required for oxidative phosphorylation (Kroemer et al., 2007). The charge imbalance that results from the

generation of the electrochemical gradient across the MIM forms the basis of the inner mitochondrial transmembrane potential ($\Delta\psi M$).

The permeability of the outer mitochondrial membrane (MOMP), which delimits the outer contour of mitochondria, is also well regulated, both in normal life and during cell death. Apparently, MOMP is freely permeable to small metabolites and solutes up to 5 kDa, due to the presence of the voltage-dependent anion channel (VDAC) protein, that would allow diffusion of this solutes. However, this view has been challenged during recent years, because real-time measurements of mitochondrial $Ca^{2+}$ concentrations revealed the control of VDAC and a variety of additional MOMP proteins to limit the diffusion of $Ca^{2+}$ (Kroemer et al., 2007).

Since, MOMP can be triggered by $Ca^{2+}$, which results in the opening of permeability transition pore made of a large proteinaceous complex. The pore opening is activated by high $Ca^{2+}$ concentration in the mitochondrial matrix, which is further stimulated by oxidative stress, pyridine nucleotide and thiol oxidation, alkalinisation and low transmembrane potential. This opening allows $Ca^{2+}$ and low molecular weight protein component to translocate from mitochondria into the cytosol. On the other hand, influx of water and solutes from the cytosol results in mitochondrial swelling and membrane rupture. The permeability transition pore formation also leads to the release of cytochrome c, AIF and other pro-apoptotic proteins from the mitochondria (Zhivotovsky & Orrenius, 2010a, 2010b; Orrenius et al., 2011)

When MMP has occurred, it leads to cell death rapidly and efficiently, through a variety of independent and redundant mechanisms. These include not only caspase activation but also the release of caspase-independent death effectors, as well as irreversible metabolic changes.

Therefore, MMP can even commit a cell to die when caspases are not activated. This "caspase-independent death" can occur because of an irreversible loss of mitochondrial function as well as because of the mitochondrial release of caspase-independent death effectors including apoptosis-inducing factor (AIF) (Kroemer et al., 2007).

Shortly after the discovery that MMP is frequently impaired in cancer, mitochondria have become an attractive target to induce apoptosis and to overcome resistance to chemotherapy. Currently, more than 20 mitochondrion-targeted compounds have been reported to induce apoptosis selectively in malignant cell lines, and some of these are already being used in phase II/III clinical trials or validated in vitro in preclinical settings (Kroemer et al., 2007).

Cancer cells are often relatively resistant to MMP induction and the inhibition of MMP constitutes an important strategy for the pharmaceutical prevention of unwarranted cell death. Conversely, induction of MMP in tumour cells constitutes the goal of anticancer chemotherapy.

(a) **Apoptotic inducing factor (AIF)**

In the absence of apoptotic stimuli, AIF resides in the intermembrane space of the mitochondria, where it co-localises with the mitochondrial chaperonin, Hsp60. However, in response to apoptotic stimuli, the 62kDa AIF is cleaved into a soluble 57kDa apoptotic protein. One of the proposed mechanisms for this cleavage is by calpain and cathepsins. Calpain activation of AIF is $Ca^{2+}$ dependent while cathepsins activate AIF in a $Ca^{2+}$ independent manner. Bax is responsible for the mitochondrial membrane permeability necessary for release of the soluble form of AIF, sAIF, from the mitochondria to the nucleus. Here, sAIF will induce chromatin condensation and high molecular weight of DNA fragmentation together with endonuclease G, an apoptotic DNase also released from mitochondria. Thus, the localisation of these proteins in the nucleus induces the

caspase-independent cell death (Kourtis & Tavernarakis, 2009).

### 2.3.4 Reactive oxygen species (ROS) and DNA damage

ROS are radicals, ion or molecules that have single unpaired electron in their outermost shell of electrons, making them highly reactive. There are two categories of ROS, the first of which is the free oxygen radicals such as superoxide ($O_2^-$), hydroxyl radical ($^-OH$), nitric oxide ($NO^-$), peroxyl radicals ($ROO^-$) and alkoxyl radicals ($RO^-$). The second category is non-radical ROS such as hydrogen peroxide ($H_2O_2$), ozone/trioxygen ($O_3$), organic hydroperoxides (ROOH) and hypochloride (HOCl). ROS typically are generated as by-products during mitochondrial electron transport in cellular respiration and in phagocytic cells through secretion of various stimuli such as TNFα. Besides that, ROS can also be produced through catalysis of NADPH oxidase, a multicomponent membrane bound enzyme complex (Phaniendra et al., 2015).

ROS have roles in a number of cellular processes such as cell cycle and programmed cell death. High levels of ROS can lead to oxidative stress, cellular damage and DNA damage depending on the severity and duration of ROS exposure. Therefore, a balance in ROS production and detoxification is important in determining the cells fate.

High generation of ROS increases cellular oxidative stress. Consequently, oxidative damage result in DNA base modifications, single- and double-strand breaks and the formation of apurinic/apyrimidinic lesions, many of which are toxic and/or mutagenic. It is hypothesised that chemotherapeutic amplification of ROS levels drives cancer cells over the threshold to induce cell death. The three most well studied ROS in cancers cells, hydroxyl radical ($^-OH$), superoxide ($O_2^-$) and hydrogen peroxide ($H_2O_2$), have all been shown to damage DNA in *in vitro* cultured cells (Barzilai & Yamamoto, 2004). There are many chemotherapeutic drugs that execute cancer cell death through ROS generation,

such as doxorubicin, daunorubicin and epirubicin (Salmon et al., 2004; Liou & Storz, 2010; Kumari et al., 2018; Srinivas et al., 2018; Yang et al., 2018;).

In summary, the first discovery of cell death induction without caspases has opened a new insight to better understand the mechanism of death in cells. After more than 30 years, there have been many studies reporting cell death independent of caspases. However, unlike the classical CD-PCD, these reports have shown that there is no definite pathway for CI-PCD. CI-PCD has been reported to go through a variety of pathways specifically depending on the death triggers and cell types. Therefore, this study is an effort to understand the CI-PCD mechanism induced by the natural coumarin analogues DMDP-1 and DMDP-2 in the prostate cancer cell lines PC-3 and DU 145.

# CHAPTER 3: METHODOLOGY

## 3.1 Cell culture

### 3.1.1 Cell maintenance

The prostate cancer cell lines PC-3 and DU 145 were purchased from American Type Culture Collection (Virginia, USA). The cells were cultured on either T-25 or T-75 cell culture flasks in RPMI 1640 (Hyclone, Massachusetts, USA) supplemented with 10% (v/v) fetal bovine serum (FBS) (Biowest, Nuaillé, France) and 1% penicillin/streptomycin (Lonza, Basel, Switzerland). Cells were cultured in a $CO_2$ incubator at 37°C with 5% $CO_2$ and 95% humidity.

### 3.1.2 Cell sub-cultivation and harvest

Cells were split every three to four days upon reaching 80%-90% confluency. Cells were rinsed with warm sterilized phosphate buffered saline (PBS) once before incubation with warm 0.25% trypsin solution diluted in PBS-ethylenediaminetetraacetic acid (EDTA) at 37°C for 7 minutes to detach cells from the flask. Trypsin activity was neutralized with 1:3 volume of trypsin to FBS supplemented media. Cells were pelleted through centrifugation at 400 × g for 5 minutes in the Eppendorf centrifuge 5702 (Eppendorf, Hamburg Germany). The supernatant was discarded and remaining pelleted cells were resuspended with supplemented media. Cells were either plated into a new cell culture flask for maintenance or counted to be used for further analysis.

### 3.1.3 Cell counting

Cell number was calculated via dye exclusion viability assay using a haemocytometer. An equal volume of harvested cell suspension was mixed with 20μL of 0.08% trypan blue stain solution (Merck Group, Darmstadt, Germany) and incubated at room temperature. After 3 minutes, 10μL of the mixture was pipetted and transferred into the haematocytometer chamber. The chamber was placed under Eclipse TS100 inverted

microscope (Nikon, Tokyo, Japan) at 10× magnification. Live cells (unstained) in the large central gridded squares (1mm) was counted. The cells concentration was calculated using the following formula:

$$Cell\ concentration\ (cell/mL) = \frac{Number\ of\ cells}{Number\ of\ grids\ counted} \times Dilution\ factor\ \times 10^4 \qquad (3.1)$$

### 3.2 Identification of $IC_{50}$ values

To identify the half maximal inhibitory concentration ($IC_{50}$) of DMDP-1 and DMDP-2, a colorimetric-based viability assay, MTT assay was used. This assay uses reduction of a yellow tetrazolium salt (3-(4,5-dimethylthiazol-2-yl)-2, 5-diphenyltetrazolium bromide (MTT) to measure the cellular metabolic activity as an indicator for cell viability. For each cell line, 200 000 cells per well were plated in a 96 -well plate and allowed to grow overnight. A column of wells was left blank as the blank control. To determine the relative number of cells for each well, a standard curve was created for every plate. A serial dilution of cells was done, starting from 200 000 cells down to 6500 cells for the standard curve reference. PC-3 and DU 145 cells were treated with different concentration of DMDP-1 and DMDP-2 (respectively) ranging from 2-25 μM for 24 hours. Media was carefully removed and replaced with 5% MTT diluted in PBS. The cells were incubated for 30 minutes at 37°C until intracellular purple formazan crystals were visible. The MTT solution was removed and DMSO as a solubilizing solution was added for 1 hour until the purple crystal was all dissolved. The absorbance was measured with a spectrophotometer (Tecan Sunrise, Germany) at 570nm wavelength.

The following formula was used to interpret the results:

$$Percentage\ of\ viable\ cells = \left(\frac{OD_{sample} - OD_{blank}}{OD_{control} - OD_{blank}}\right) \times 100 \qquad (3.2)$$

Based on the data collected, a linear graph was created, the $IC_{50}$ was determined through the graph.

## 3.3 Cell treatment

### 3.3.1 Plant Materials

The bark of *Mesua elegans* (King) Kosterm was collected from Sungai Badak Forest Reserve, Kedah, Malaysia. The sample was identified by Mr. Teo Leong Eng and deposited in the Department of Chemistry, Faculty of Science, University of Malaya herbarium (Ref. No: KL5232). Geranylated 4-phenylcoumarin analogues DMDP-1 and DMDP-2 were extracted and with ≥ 98% purity from the bark using high performance liquid chromatography by Mr. Fadzli Bin Md Din, Department of Chemistry, Faculty of Science, University of Malaya.

### 3.3.2 Pharmacological inhibitors

Calpain-2 inhibitor, calpeptin and cathepsin B activity inhibitor ≥ 99%, CA-074, were purchased from Merck (Darmstadt, Germany).

### 3.3.3 Treatment with compound analogues

PC-3 cells were treated with DMDP-1 at $IC_{50}$ of 13μM, while DU 145 cells were treated at $IC_{50}$ of 5μM. The prostate cancer cells were plated onto a new cell culture flask one day prior to treatment. On the day of treatment, old media supplemented with FBS was discarded and replaced with a warm un-supplemented media. Next, DMDP-1 and DMDP-2 were added to PC-3 and DU 145 cell lines following their respective $IC_{50}$ value.

### 3.3.4 Treatment with inhibitors

The concentration for inhibitor used for treatment was 30mM for calpeptin and 10mM for CA-0714. The cells preparation was similar to treatment with compounds (Chapter 3.3.3), however, after replacement of new un-supplemented media, the inhibitors were added first, four hours before addition of the compound analogues into the cell culture.

## 3.4 Protein extraction

All untreated and DMDP-1&-2 treated PC-3 and DU 145 cells were harvested with trypsinization and centrifugation at 400 × g for 5 minutes prior to extraction.

### 3.4.1 Cytoplasmic protein extraction

The cytoplasmic proteins were extracted from cells using NE-PER1 Nuclear and Cytoplasmic Extraction Kit (Thermo Fisher Scientific, Massachusetts, USA) mixed with Halt Protease Inhibitor Cocktail (Thermo Scientific, Massachusetts, USA). Harvested cells were rinsed with PBS and centrifuged at 500 × g for 5 minutes to pellet the cells in a 1.5mL microcentrifuge tube. The supernatant was carefully removed by pipetting, leaving approximately 10μL of cell pellet. Ice cold CER I was added to the cell pellet, and the mix was vortexed vigorously on the highest setting to fully suspend the cell pellet. The tube containing the mix was incubated on ice for 10 minutes. Next, 5.5 μL ice-cold CER II was added to the tube and vortexed at highest setting for 5 seconds. The tube was incubated on ice for 1 minute before vortexed again for another 5 seconds at the highest setting. Finally, the mix was centrifuged for 5 minutes at 16000 × g. The cytoplasmic extract in the supernatant was immediately transferred to a fresh pre-chilled microcentrifuge tube and placed on ice until further use.

### 3.4.2 Mitochondrial protein extraction

#### 3.4.2.1 Mitochondrial isolation

Mitochondria was isolated using the Mitochondrial Isolation Kit for Cultured Cells (Thermo Fisher Scientific, Massachusetts, USA) mixed with Halt Protease Inhibitor Cocktail (Thermo Scientific, Massachusetts, USA). A total of $2 \times 10^7$ cells were harvested and mixed with 800 μL of mitochondrial Isolation Reagent A in a 2 mL microcentrifuge tube. The mix was vortexed at medium speed for 5 seconds and incubated on ice for 2 minutes. Then, 10 μL of Mitochondrial Isolation Reagent B was added to the mix and vortexed at maximum speed for 5 seconds. The tube was incubated on ice for 5 minutes and vortexed at maximum speed every minute. Next, 800 μL of Mitochondrial Isolation reagent C was added to the tube and mixed by inverting the tube several times. The mixture was centrifuged at 700 × g for 10 minutes at 4°C. The supernatant was then transferred into a new 2mL tube and centrifuged at 12000 × g for 15 minutes at 4°C. The supernatant was discarded and the cell pellet containing isolated mitochondria was washed by adding 500 μL Mitochondrial Isolation C and centrifuged at 12000 × g for another 5 minutes. The supernatant was discarded and the purified mitochondria in the pellet were placed on ice for mitochondrial lysis.

#### 3.4.2.2 Mitochondrial protein extraction

The mitochondrial protein extraction was done using RIPA Extraction and Lysis buffer (Thermo Fisher Scientific, Massachusetts, USA). The isolated mitochondria were resuspended in 100 μL of the buffer (mixed with 1:100 protease inhibitor: RIPA buffer) and placed on ice for 10 minutes for lysis. Next the mitochondria-RIPA buffer mix was centrifuged at 16000 × g for 10 minutes. The supernatant containing the mitochondrial

protein extract was collected and transferred into a new tube on ice for immediate analysis.

### 3.4.3 Nuclear protein extraction.

The nuclear proteins were extracted based on the two-minute cell fractionation method-REAP (Suzuki et al., 2010). Harvested cells were counted to standardise the cell numbers of each sample before lysis in 0.1% NP40 alternative (Merck, Darmstadt, Germany) in PBS for 30 seconds. Subsequently, the lysed cells were centrifuged at the highest speed (16000 × g) for 10 seconds. The pellets collected were resuspended in 0.1% NP40 alternative for 30 seconds and centrifuged at the highest speed for another 10 seconds to obtain the final pellets containing the nuclear fractions.

## 3.5 Western Blot

### 3.5.1 Sample preparation

#### 3.5.1.1 Protein quantification

All extracted protein fractions were measured with spectrophotometer Nanodrop 2000 (Thermo Fisher Scientific, Massachusetts, USA) at 562 nm wavelength according to protein quantification kit from PierceTM BSA Protein Assay Kit (Thermo Fisher Scientific, Massachusetts, USA). A standard curve for protein concentration was established with bovine serum albumin (BSA) at concentrations of 25, 125, 250, 500, 500, 750, 1000, 1500, and 2000 μg/mL. Each protein sample was mixed with 200 μL of the BCA working reagent mix (50 part of reagent A: 1 part of Reagent B) for measurement. Based on the absorbance, the protein concentration was determined by referring to the standard curve.

#### 3.5.1.2 Protein denaturation

Once the protein concentration was determined, 40 μg of proteins from each sample was diluted to a total volume of 20 μL with $dH_2O$ and 5× Lane Marker Reducing Sample Buffer (Thermo Fisher Scientific, Massachusetts, USA) containing dithiothreitol (DTT) and SDS to denature and induce uniform charge-to-mass ratio to the protein sample. The samples were heated for 5 minutes at 95°C with a heat block MiniT-100 (AOSheng, China). Concurrently, biotinylated protein ladder (Cell Signalling Technology, Massachusetts, USA) was heated at 95°C for 2 minutes. Next, the heated samples and ladder were allowed to cool down in room temperature before loading into the gel.

### 3.5.2 Sodium dodecyl sulfate - polyacrylamide gel electrophoresis (SDS-PAGE)

Protein separation was done based on sizes with SDS-PAGE. The gel consisted of two layers of different percentages of polyacrylamide, which were the stacking gel (top layer) and resolving gel (bottom layer). Based on the molecular weight of the proteins of interest, different percentages of resolving gel were used for the protein separation, in which smaller proteins ranging from 10-70kDa were ran on 10% (w/v) gel while larger proteins of 24kDa-200kDa on 7.5% (w/v) of gel, with the percentage for stacking gel being the same in all experiment at 4% (w/v). Table 3.1 shows the ingredients used to prepare the gels.

**Table 3.1: Ingredients for SDS-polyacrylamide gel**

| Ingredient | Stacking gel 4% (μL) | Resolving gel 7.5% (μL) | Resolving gel 10% (μL) |
|---|---|---|---|
| Distilled water ($dH_2O$) | 3180.0 | 8200.0 | 7270.0 |
| 0.5M Tris-HCl (pH 6.8) | 1250.0 | - | - |
| 1.5M Tris-HCl (pH 8.8) | - | 2500.0 | 3750.0 |
| 10% SDS | 50.0 | 150.0 | 150.0 |
| 40% Acrylamide (Promega, Wisconsin, USA) | 500.0 | 2820.0 | 3750.0 |
| 10% (w/v) Fresh ammonium persulfate (APS) | 25.0 | 75.0 | 75.0 |
| Tetramethyl-ethylenediamine (TEMED) (Acros, Massachusetts, USA) | 5.0 | 7.5 | 7.5 |
| Bromophenol blue | 10.0 | - | - |
| Total volume | 5000.0 | 15000.0 | 15000.0 |

To cast the gel, glass plates of 1 mm thickness and 18 cm × 16 cm dimension (Bio-Rad Laboratories, CA, USA) were set into the provided casting tray. Approximately 5.0mL of the resolving gel mix was gently pipetted into the space between the glass plates until the solution occupied three quarters of the whole space. A thin layer of 0.1% SDS diluted in PBS was added on top of the resolving gel to ensure an even surface layer. After the gel solidified, the 0.1% SDS-PBS solution was removed and the stacking gel mix was added on top of the resolving gel until the whole space was filled. A 10 wells-comb was added into the gel and left for 40 minutes to solidify.

The solidified gels were transferred into the Mini PROTEAN Tetra System (Bio-Rad Laboratories, California, USA). The tank was filled with Tris/Glycine/SDS (TGS) running buffer and connected to the electrophoresis power source Power Pack (Bio Rad, California, USA). The comb was removed and 20μL of protein samples and 8μL of biotinylated protein ladder control were loaded into the respective wells. After loading, electrophoresis was carried out at 110 volts and a maximum of 400mA for 15 minutes, followed by 150 volts and a maximum of 400 mA for another 40 minutes or until the bright pink dye of the sample buffer had reached the bottom of the gels.

### 3.5.3 Protein transfer

After the electrophoresis, the separated proteins were transferred to 0.22 μM nitrocellulose membranes (Bio-Rad, California, USA) for immunoblotting. The gels were carefully taken out from their casts and soaked in the transfer buffer (TGS mixed with 20% methanol) for 10 minutes together with the nitrocellulose membrane and filter paper (Bio-Rad, California, USA). The proteins transfer was done via the semi-dry transfer method, using Trans-Blot SD Semi-Dry Transfer Cell (Bio-Rad, California, USA). The filter papers were arranged to sandwich the nitrocellulose membrane and the gel. The transfer was run at 50 mA and 25 volts for every gel used for 90 minutes using MP-2AP Power Supply (Major Science, Taiwan). Next, to visualize the proteins transferred onto the nitrocellulose membrane, the membranes were stained with Ponceau S (Merck Group, Darmstadt, Germany). Once the protein transfer was confirmed by the visibility of the protein bands, the stain was rinsed off with distilled water. The membrane was then incubated with blocking buffer on a shaker for one hour. The blocking buffer was rinsed off the membrane with TBST for 10 seconds before proceeding to the immunoblotting steps.

### 3.5.4 Immunoblotting

Immunoblotting was done by incubating the membranes with primary antibody overnight at 4°C followed by incubation with horseradish peroxidase (HRP)-linked secondary antibody. To visualise the target proteins, 8 primary antibodies against calpain-2, cathepsin B, GRP-78/Bip, p-eIF2 alpha, apoptotic inducing factor (AIF), GAPDH, H2B and Cox IV (Cell Signaling Technology, Danvers, USA) were used. After the overnight incubation, the membranes were incubated for an additional hour on a shaker at room temperature. Next, the membranes were washed three times with TBST, 5 minutes for each wash. Incubation with secondary antibody consisting of biotin-

conjugated anti-rabbit antibodies was done for an hour on a shaker at room temperature. After washing the membranes 3 times with TBST, the protein bands were detected through chemiluminescence by exposing the membrane to WesternBright Quantum (Advansta, USA) prior to visualisation with a chemiluminescent imaging system (Fusion FX7). GAPDH, Cox IV and H2B were used for normalisation of band intensity for cytoplasmic, mitochondrial and nuclear fractions respectively by using a densitometry sofware imageJ v1.48 (NIH, USA).

### 3.6 Intracellular calcium measurement

For each untreated and DMDP-1 & -2 treated PC-3 and DU 145 sample, a total of $4 \times 10^6$ cells was harvested with trypsinization and spun down at 400 × g for 5 minutes. The measurement of the intracellular calcium concentration was done as recommended and following the protocol from a calcium measurement kit QuantiChromeTM Calcium Assay Kit (BioAssay, USA) as follows.

#### 3.6.1 Cell lysis

Harvested cells were lysed with a sonicator. The cell pellet was resuspended in PBS and sonicated at 2 level of speed for 5 seconds and put on ice for 5 seconds. These steps were repeated for 3 times. Finally, the pellet was centrifuged for 3 minutes at 400 × g, and the supernatant was collected for analysis.

#### 3.6.2 Intracellular calcium measurement

The working reagent was prepared by combining the equal volume of reagent A and reagent B of QuantiChromeTM Calcium Assay Kit in sufficient amount for the standards and samples. The standard was set up to range from 20mg/dL to 0mg/dL for standard curve generation. For each sample, 5μL was mixed with (volume?) of working reagent and incubated for 3 minutes at room temperature before measuring the optical density

with spectrophotometer (Tecan Sunrise) at 570-650nm (peak absorbance at 612nm). The calcium concentration was determined with the following formula:

$$[Ca^{2+}] = \frac{\frac{OD_{sample}}{OD_{blank}}}{Slope\ ^{mg}/_{dL}} \quad (3.3)$$

### 3.7 Cathepsin B activity measurement

All untreated and DMDP-1&-2 treated (24 hr) PC-3 and DU 145 cells were harvested with trypsinization and centrifuged at 400 × g for 5 minutes prior to measurement. Cathepsin B activity was measured following the protocol from a cathepsin B activity measurement kit Magic Red™ Cathepsin assay kit. The harvested cells were counted and $1\times 10^5$ of cells were transferred into each well of a 96-well sterile black plate. The cells were incubated with the fluorescent staining solution Magic Red for an hour at 37°C, protected from light. Then, the fluorescence intensity was measured by a microplate reader at 592 nm and 628 nm excitation and emission wavelength, respectively.

### 3.8 Reactive oxygen species detection

Untreated and DMDP-1&-2 treated PC-3 and DU 145 cells were harvested with trypsinization and centrifuged at 400 × g for 5 minutes at room temperature prior analysis. Reactive oxygen species (ROS) detection was done following the protocol of Cellular ROS/Superoxide Detection Assay Kit (Abcam, USA). Firstly, the harvested cells were rinsed with the provided wash buffer before being resuspended with ROS/Superoxide Detection solution containing the fluorescent dyes. After incubation in the dark for 30 minutes at room temperature, the generated fluorescent products were measured using flow cytometer equipped with a blue laser (488 nm filter).

### 3.9 DNA damage by oxidative stress detection

The DNA damage by oxidative stress was detected by monitoring the formation of the damage by-product which is 8-hydroxy-oxyguanosine (8-OHdG).

Both PC-3 and DU 145 cells were plated on 24-well plates and treated with the analogues at their respective $IC_{50}$ values. Cells were fixed with 4% formaldehyde-PBS, rinsed with PBS before being incubated in a blocking buffer of 1× PBS/5% normal serum/0.3% Triton™ X-100 for 1 hour in room temperature. Blocking buffer was removed and incubated with primary antibodies: mouse monoclonal antibody against 8-hydroxy-oxyguanosine (8-OHdG) (Santa Cruz Biotechnology, USA) at 4° C overnight. Subsequently, the cells were rinsed with PBS and incubated with secondary antibodies of Goat anti-Mouse IgG H&L (Alexa Fluor® 488) (Abcam, USA) for one hour in room temperature before observed under fluorescent microscope.

# CHAPTER 4: RESULTS

## 4.1 Identification of DMDP-1 and DMDP-2 $IC_{50}$ values in PC-3 and DU 145 cell lines, respectively

MTT assay was carried out to elucidate the cytotoxic effects and determine the $IC_{50}$ values of the analogues in prostate cancer cell lines. The $IC_{50}$ values for DMDP-1 in PC-3 is 13µM, while DMDP-2 in DU 145 is 5µM. The $IC_{50}$ values were used for the treatment of PC-3 and DU 145 throughout this study.

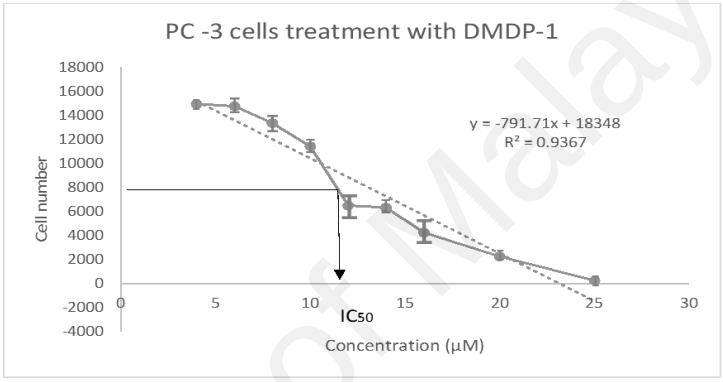


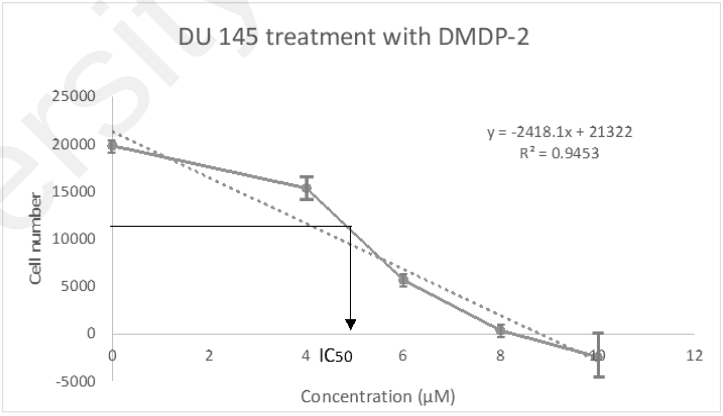


**Figure 4.1:** DMDP-1 and DMDP-2 $IC_{50}$ value. MTT assay was used to determine the $IC_{50}$ of DMDP-1 and DMDP-2 in PC-3 and DU 145 cells respectively. Results were presented as mean normalised intensity ± standard deviation (S.D.) of three independent experiments

## 4.2 Disruption of intracellular homeostasis and calpain-2 activation

One of the key factors of cell survival is the ability of the cell to maintain its intracellular homeostasis. Any damages or insults could trigger disruption in the intracellular balance which if left unfixed would lead to cell death. Therefore, it is important to observe the intracellular homeostasis in investigating cell death mechanisms. In this study, the changes in two intracellular homeostasis parameters investigated were calcium ion ($Ca^{2+}$) level and endoplasmic reticulum (ER) stress level.

### 4.2.1 Elevation in intracellular $Ca^{2+}$ level

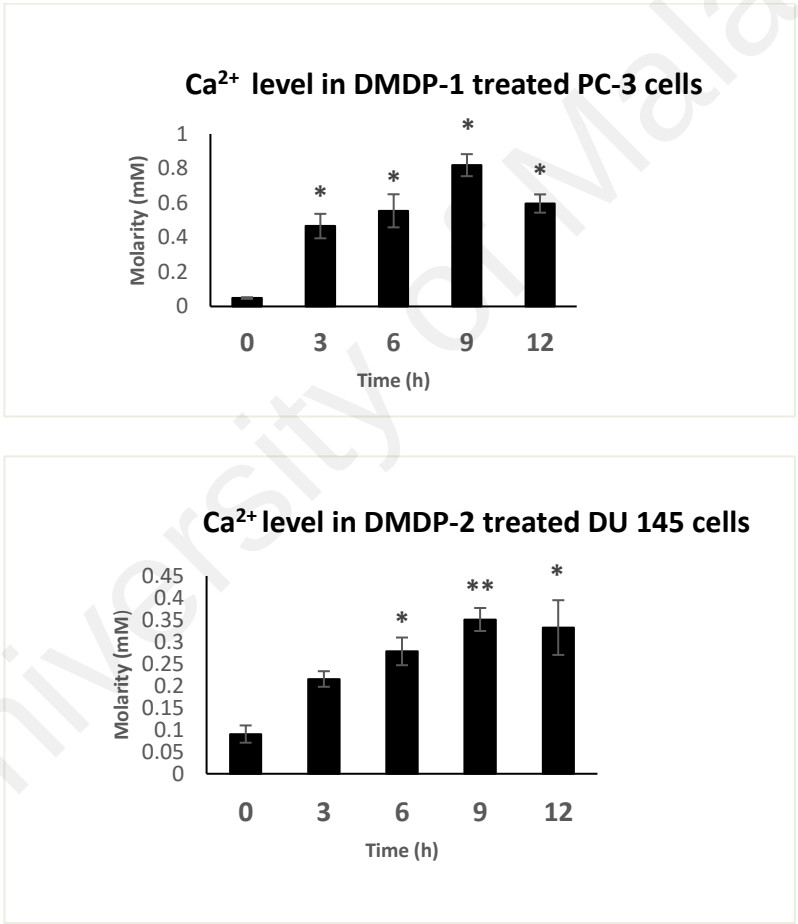


**Figure 4.2:** Calcium level of PC-3 and DU 145 cells. The $Ca^{2+}$ levels in DMDP-1 treated PC-3 and DMDP-2 treated DU 145 were measured without treatment at 0 h and at 3, 6, 9 and 12 h of treatment. Significant increases were observed as early as 3 h of treatment in both cell lines compared to 0 h. Results were presented as mean normalized intensity ± S.D. of three independent experiments. (*) denotes $p < 0.05$, and (**) denotes $p < 0.005$.

A colorimetric assay (Figure 4.2) was carried out to measure the alteration in the intracellular $Ca^{2+}$ level in PC-3 and DU 145 upon treatment with DMDP-1 and DMDP-2 respectively. In this assay, the phenolsulphonethalein dye formed a stable blue coloured complex specifically with free $Ca^{2+}$ in the samples. The intracellular $Ca^{2+}$ levels of both cell lines were measured without treatment at 0 hour (h) and at 3, 6, 9 and 12 h of treatment. The results obtained were analysed and significant increases were observed as early as 3 h of treatment in both cell lines in comparison to 0 h.

### 4.2.2 Endoplasmic reticulum (ER) stress and calpain-2 activation

The ER balance in the cells that undergo stressful conditions may be disrupted due to the accumulation of misfolded proteins in the ER lumen, a response named as ER stress. To determine if DMDP-1 & -2 induced significant stress into the cells, the cellular ER stress level was measured by monitoring the expression level of its markers, phosphorylated eukaryotic initiation factor (p-eIF2α) and glucose-regulated protein 78 (GRP 78). The expression levels of p-eIF2α and GRP 78 were monitored with western blotting without treatment at 0 h and at 3, 6, 9 and 12 h of treatment. In DMDP-1 treated PC-3, p-eIF2α showed a significant increase at 9 and 12 h and in DMDP-2 treated DU 145 cells at 6, 9 and 12 h. Meanwhile, GRP 78 levels were significantly increased at 6, 9 and 12 h of treatment in comparison to 0 h in both cell lines.

A

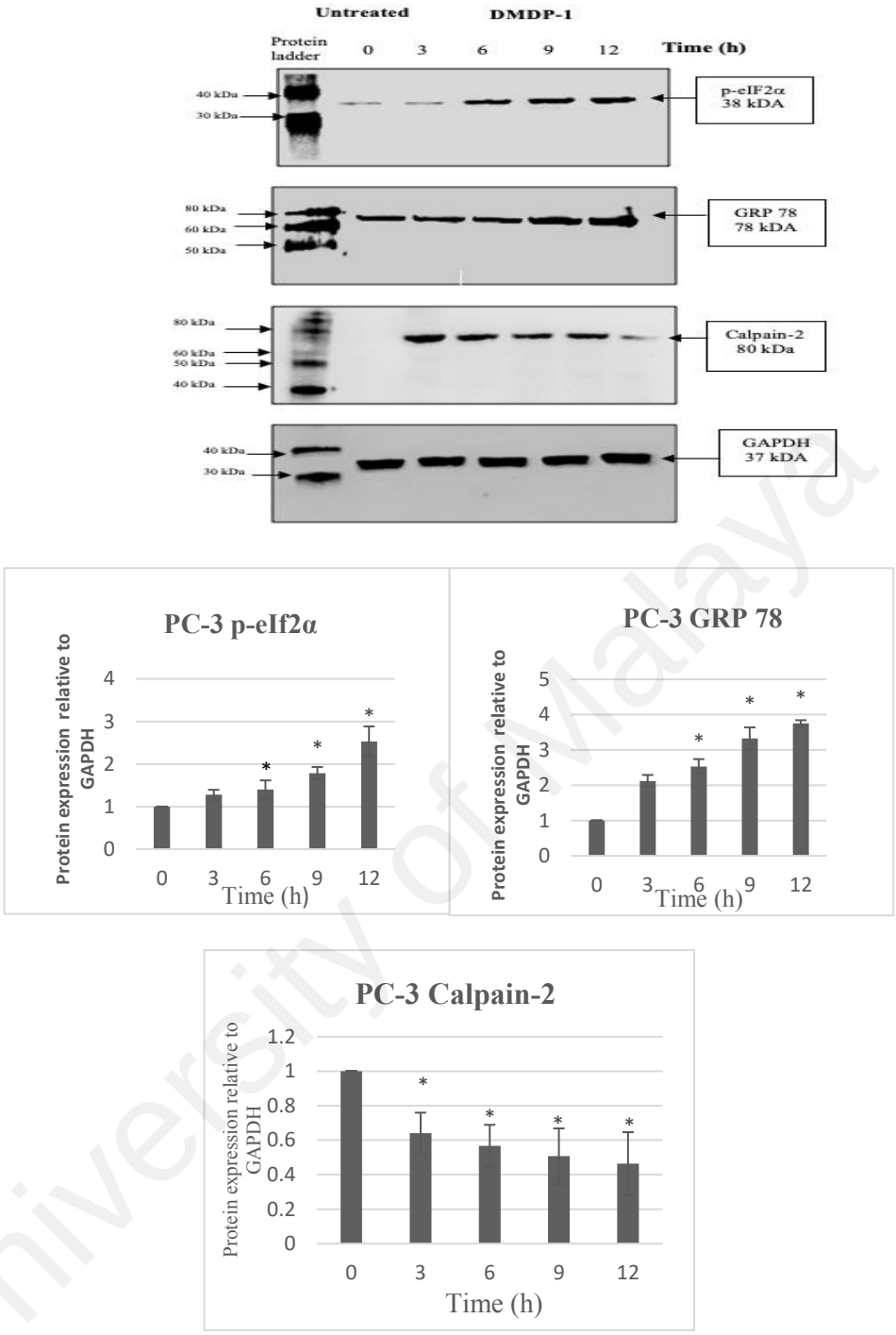


**Figure 4.3:** ER stress level and activation of calpain-2 of PC-3 and DU 145 cells. Comparative analysis was done to measure the ER stress level and calpain-2 activation in PC-3 (A) and DU 145 (B) cells. Levels of ER stress marker proteins, p-eIF2α and GRP 78, and calpain-2 autolysis were measured in western blot, with GAPDH as the housekeeping protein control. Quantification of protein bands intensities of the respective cell lines were determined by densitometry analysis and protein of interests were normalised to GAPDH using the image J v1.43 software. Results were presented as mean normalised intensity ± S.D. of three independent experiments and (*) denotes $p < 0.05$.

B

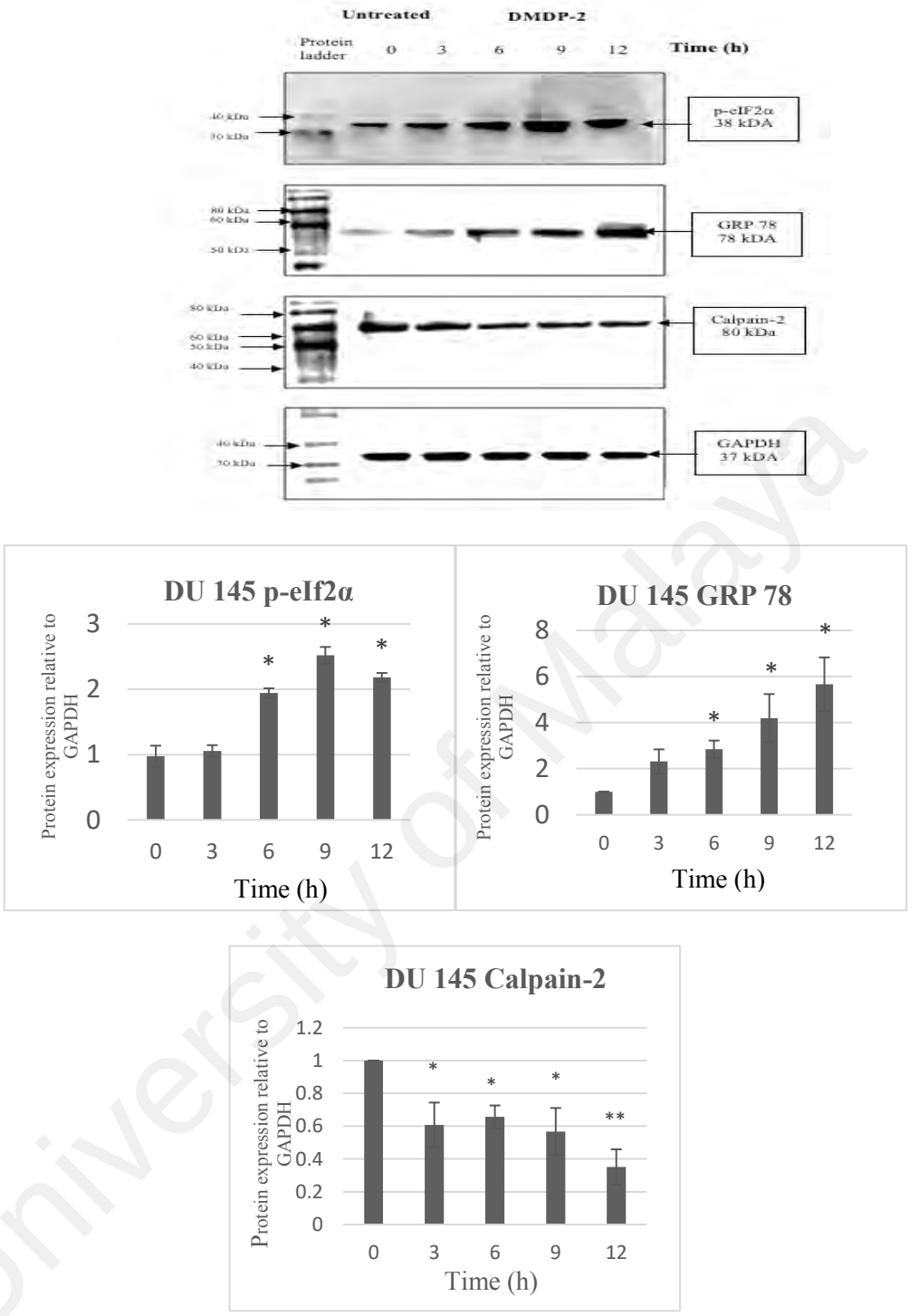


**Figure 4.3,** continued.

Calpain-2 was observed to be activated in both prostate cancer cell lines when treated with the respective analogues at 24 h in a previous study(Suparji et al., 2016). Both PC-3 and DU 145 were treated with DMDP-1 & -2 respectively for 3, 6, 9 and 12 h and then compared with untreated cells at 0 h in a western blot. As calpain-2 is auto-degraded upon

activation, a decrease in expression as early as at 3 h of treatment was observed consistently up to 12 h of treatment in both cell lines.

### 4.3 Cathepsin B activation

Another protease that has the ability to induce CI-PCD is cathepsin B. To investigate cathepsin B activity in PC-3 and DU 145 after treatment with DMDP-1 and DMDP-2 respectively, an enzyme-substrate assay detection kit Magic Red was used.

In DMDP-1 treated PC-3 cells (Figure 4.4 A), a significant increase in cathepsin B activity indicated by the fluorescence intensity was observed when compared with untreated PC-3. However, in DU 145 cells treated with DMDP-2 (Figure 4.4 B), only a slight increase in fluorescence was observed in comparison with the untreated DU 145 cells. This may be due to an existing high basal level of cathepsin B activity in the untreated DU 145 cells, which makes the DMDP-2 treatment increase insignificant. This observation was further supported when co-treatment of DU 145 untreated cells with cathepsin inhibitor, CA 075 showed a significant reduction in cathepsin B activity (Figure 4.4 C).

A

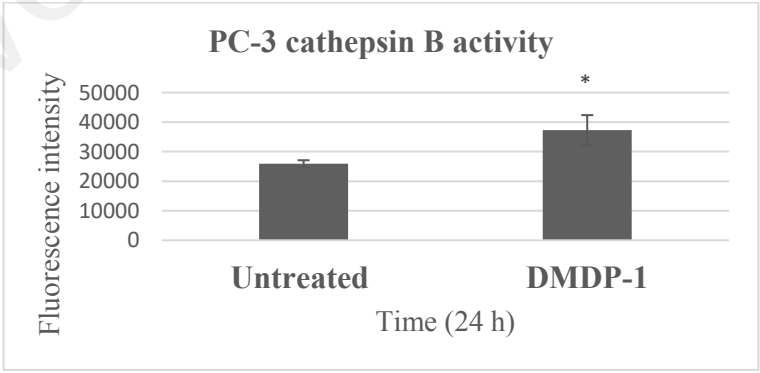


**Figure 4.4**: Cathepsin B activity in PC-3 and DU 145 cells. Comparative analysis of cathepsin B activity in (A) PC-3 and (B) DU 145 cells with and without treatment with DMDP-1 & -2 measured with enzyme-substrate assay. (C) Cathepsin B inhibitor, CA 074 was used to investigate the basal level of cathepsin B activity in DU 145 cells. Results were presented as mean normalised intensity ± S.D. of three independent experiments and (*) denotes $p < 0.05$.

B

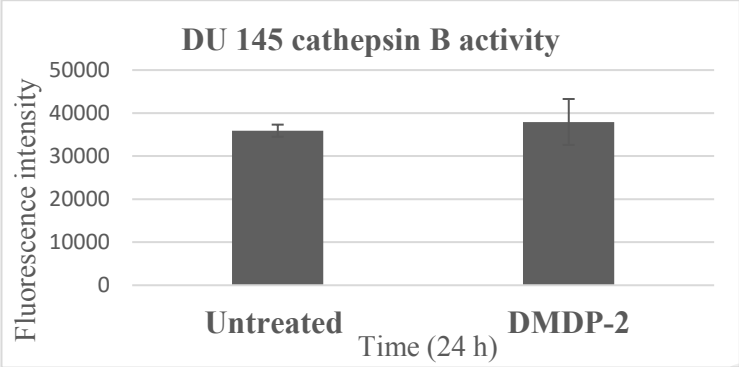


C

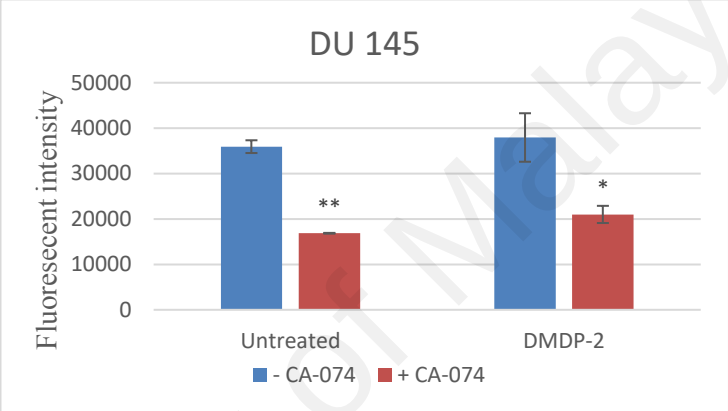


**Figure 4.4,** continued.

## 4.4 Involvement of mitochondria

### 4.4.1 Mitochondrial transmembrane potential (ΔψM) reduction

$Ca^{2+}$ level change in cells is able to affect the ΔψM. To observe if there were any changes in the ΔψM in PC-3 and DU 145 cells upon treatment with DMDP-1 & -2, respectively, flow cytometry was carried out. MMP was measured with JC-1, a potential-dependent fluorescent stain, indicated by the emission shift from green (~529 nm) to red (~590 nm) detected with flow cytometry, where a decrease in the red/green intensity ratio is an indication of an increase in MMP, measured using ΔψM. Upon treatment, JC-1 green stained cell count increased in PC-3 and DU 145 cells. The ΔψM of DMDP-1 treated PC-3 cells increased as indicated by the decrease in the ratio, 0.57±0.2 compared to the

untreated cells at 1.03±0.4. Similarly, in DMDP-2 treated DU 145 cells, the ΔψM ratio was 0.46±0.04 compared to the untreated cells at 0.98±0.07. These observations suggested there were depolarisations of the mitochondrial membrane and occurrence of MMP in both PC-3 and DU 145 cells upon treatment with the analogues DMDP-1 and DMDP-2 respectively.

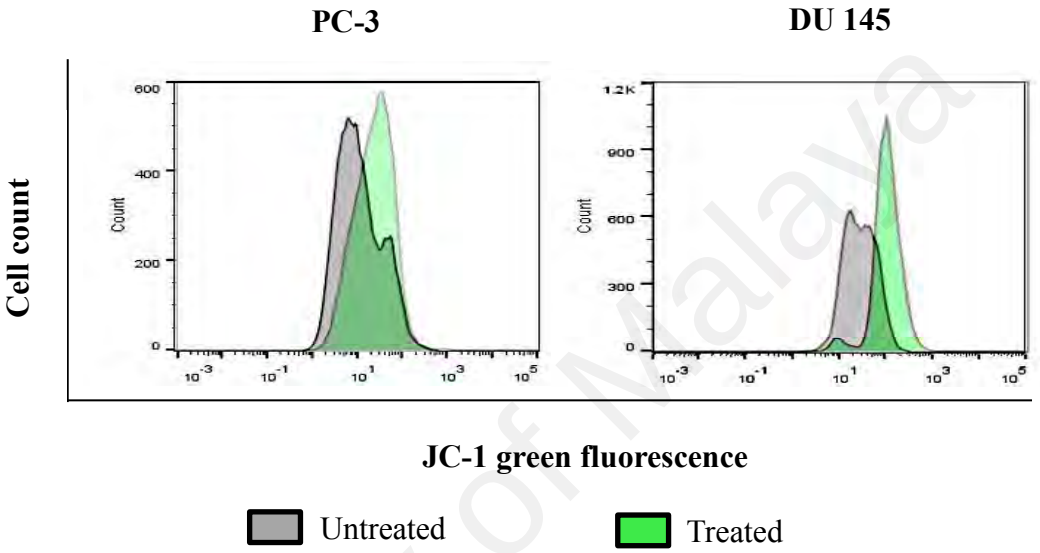


**Figure 4.5:** The mitochondrial membrane potential ΔψM) of PC-3 and DU 145 cells. The mitochondrial membrane potential (ΔψM) of PC-3 and DU 145 treated with DMDP-1 & -2 respectively was measured with flow cytometry and JC-1 as the potential-change indicator.

### 4.4.2 Apoptotic inducing factor (AIF) translocation

A mitochondrial protease, apoptosis-inducing factor (AIF) is known to participate in the regulation of mitochondrial membrane permeabilisation. AIF is a protease which, in its mature form (62kDa), is sequestered behind the outer mitochondrial membrane. It has the ability to induce cell death independent of caspases by translocating into the cytoplasm and subsequently into the nucleus, triggering chromatin condensation and large DNA fragmentation (50kbp). Changes in mitochondrial membrane potential indicate disruption of the MMP. Therefore, the involvement of AIF was investigated by monitoring the translocation of the protease. The mitochondrial AIF is truncated to form a soluble AIF (tAIF, 57kDa) to enable the translocation of tAIF into the cytoplasm and

nucleus. To study the role of AIF in the cell death induced by DMDP-1 & -2 in PC-3 and DU 145 cells respectively, the expressions of AIF in mitochondria, cytoplasm and nucleus were observed through western blotting. Both PC-3 and DU 145 cells treated with their designated analogues showed a reduction in the mitochondrial 62 kDa AIF expression after 24 h of treatment. Observations of increased 57kDa tAIF expression in the cytoplasm were made in both cell lines after treatment with the analogues (Figure 4.6). However, no expression of AIF was detected in the nucleus in both cell lines.

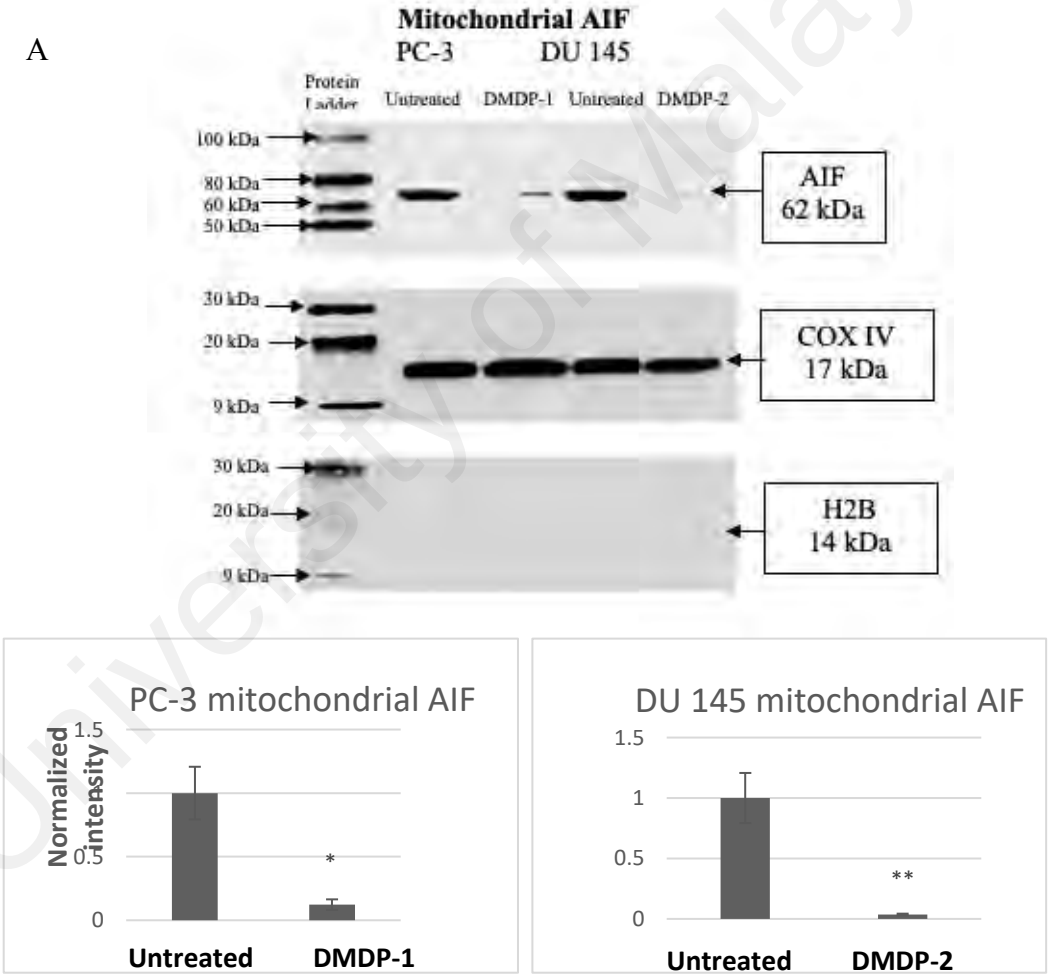


**Figure 4.6:** AIF translocation analysis. Western blot analysis to investigate the AIF translocation between organelles in the cells. Quantification of protein bands intensities were determined by densitometry analysis with image Jv1.43 software. Protein of interests were normalised to COX IV for mitochondrial with histone H2B protein as extract purity control (A), while for cytoplasmic protein normalised to GAPDH and COX IV as the extract purity control (B). Results were presented as mean normalised intensity ± S.D. of three independent experiments. (*) denotes $p < 0.05$ and (**) denotes < 0.005.

B

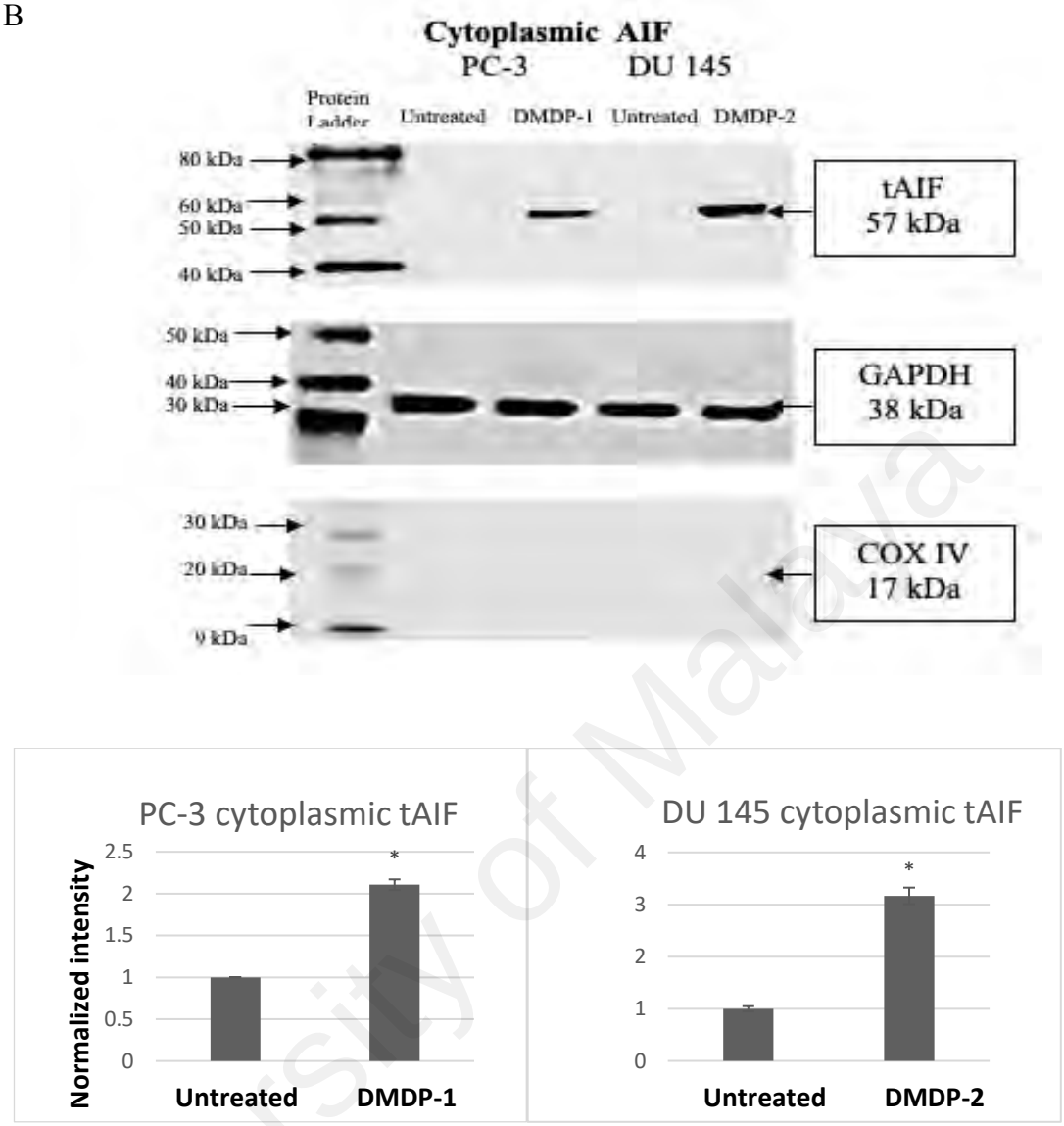


**Figure 4.6,** continued.

## 4.5 DNA damage by reactive oxygen species (ROS)

### 4.5.1 Increase reactive oxygen species (ROS) level

In the preliminary study, DNA laddering, a hallmark for CD-PCD, was not shown in both PC-3 and DU 145 treated with the analogues. Therefore, other modes of DNA damage were investigated. Since calpain-2, cathepsin B, AIF and the reduction of $\Delta\psi M$ are known to have roles in inducing ROS level in cells, increase of ROS level was investigated using flow cytometry. Both PC-3 and DU 145 cells, treated and untreated,

were stained using ROS detection kit (Abcam, USA) and analysed with flow cytometry. Results of DMDP-1 treated PC-3 and DMDP-2 treated DU 145 (Figure 4.7 A) showed a significant increase in cells containing superoxide ($O_2^-$) (shown in gate Q1), a species of ROS, in comparison with the untreated controls. Interestingly, other ROS showed no significant changes after treatment in both cell lines.

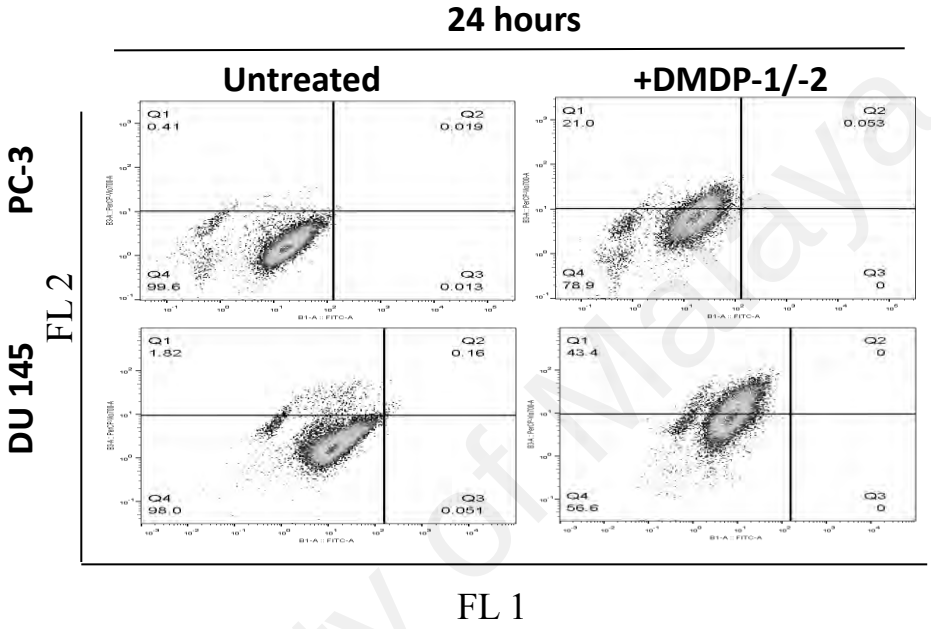


B

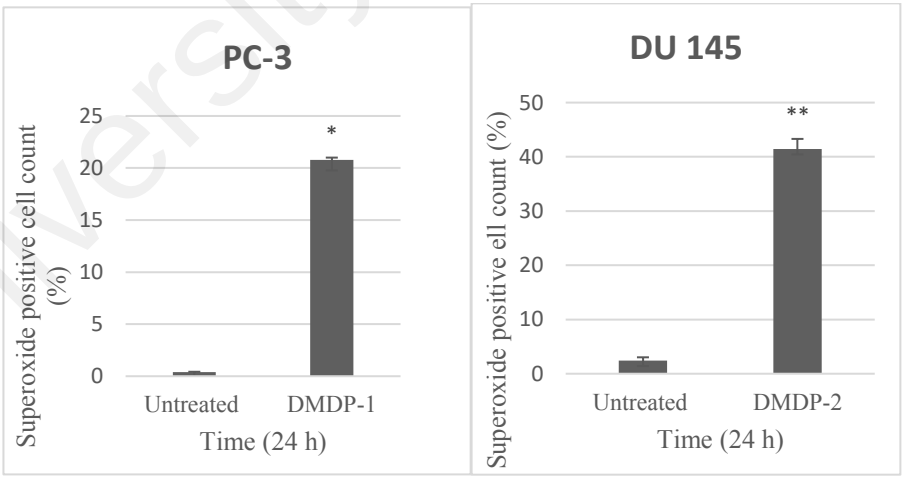


**Figure 4.7:** ROS level in PC-3 and DU 145 cells. A. Comparison analysis with flow cytometry to investigate the ROS level in PC-3 and DU 145 cells with and without treatment with the analogues DMDP-1 & -2 respectively. FL 1: Orange; FL 2: Green. B. Quantification of the cell difference between untreated and treated cells positive to superoxide ($O_2^-$) stain represented in bar chart. Results were presented as mean normalised intensity ± S.D. of three independent experiments. (*) denotes $p < 0.05$ and (**) < 0.005.

### 4.6 DNA damage by ROS detection

Significant increase in ROS formation after treatment with DMDP-1 & -2 in both cell lines suggested the possibility of DNA damage by oxidative stress due to the accumulation of ROS. Therefore, DNA damage by oxidative stress was monitored through an immunofluorescence assay detecting 8-hydroxy-oxyguanosine (8-OHdG) as the marker. Both PC-3 and DU 145 showed a significant increase in cells with DNA damage as indicated by the 8-OHdG stained cells in comparison to the untreated cells after 24 hours of treatment.

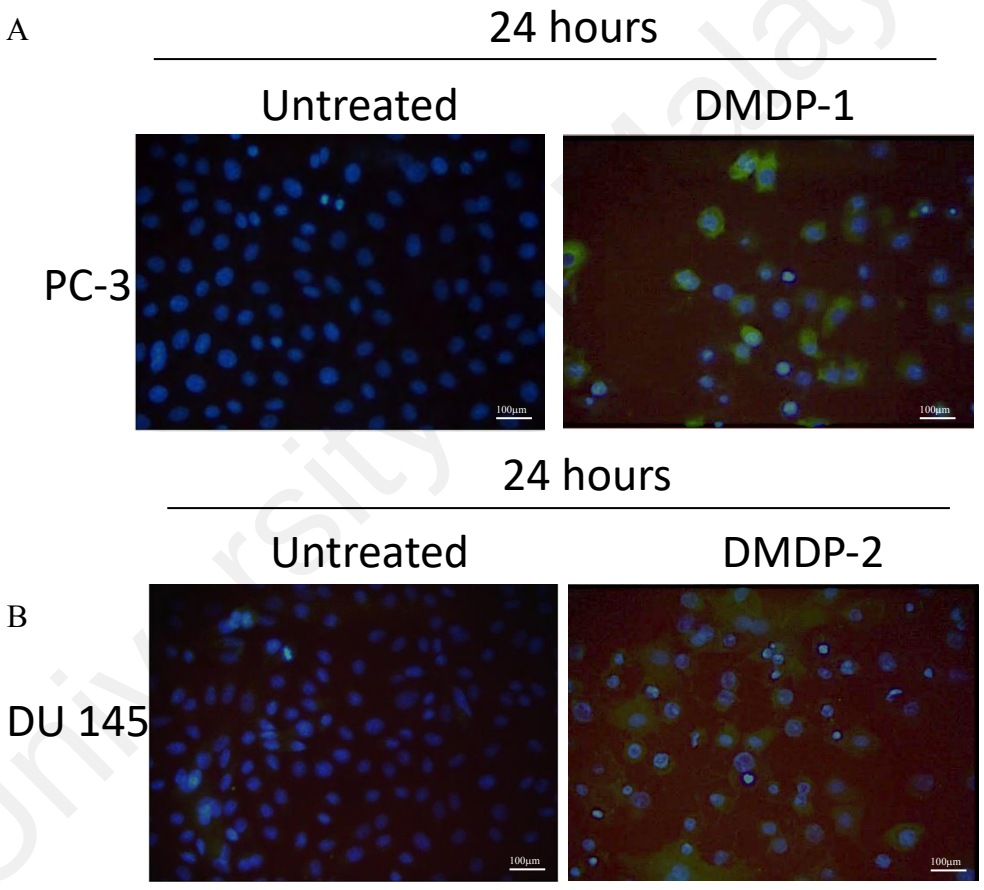


**Figure 4.8:** DNA damage by oxidative stress in PC-3 and DU 145 cells. Comparative image analysis of DNA damage by oxidative stress with immunofluorescence assay between the untreated and treated PC-3 and DU 145 cells. The marker 8-hydroxy-oxyguanosine (8-OHdG) is shown stained in green while blue DAPI was used to stain cell nucleus (A). C. The results were quantified as fluorescent relativity index represented in bar chart. Results were presented as mean normalised intensity ± S.D. of three independent experiments. (*) denotes $p < 0.05$ and (**) denotes < 0.005.

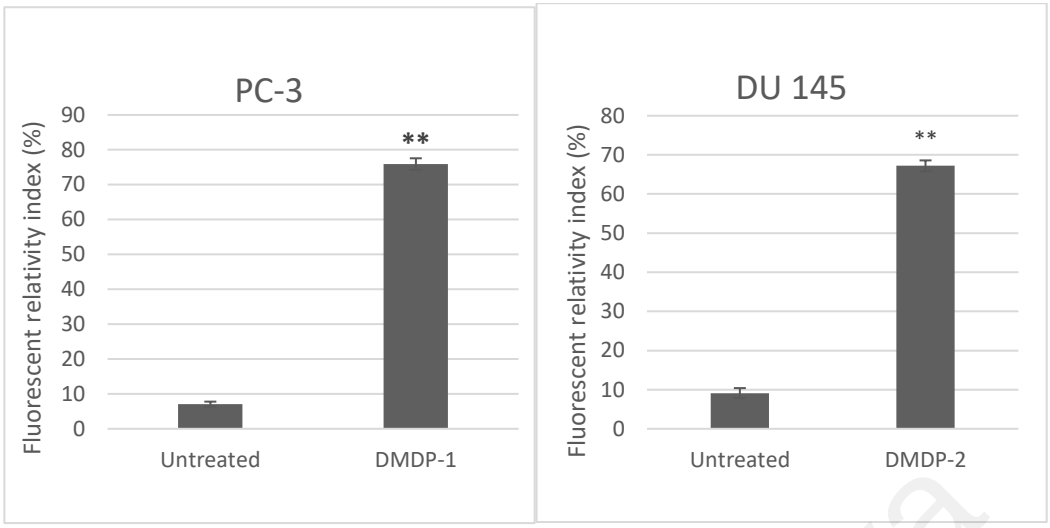


**Figure 4.8,** continued.

## 4.7 Relationship between calpain-2 and cathepsin B in the cell death induced

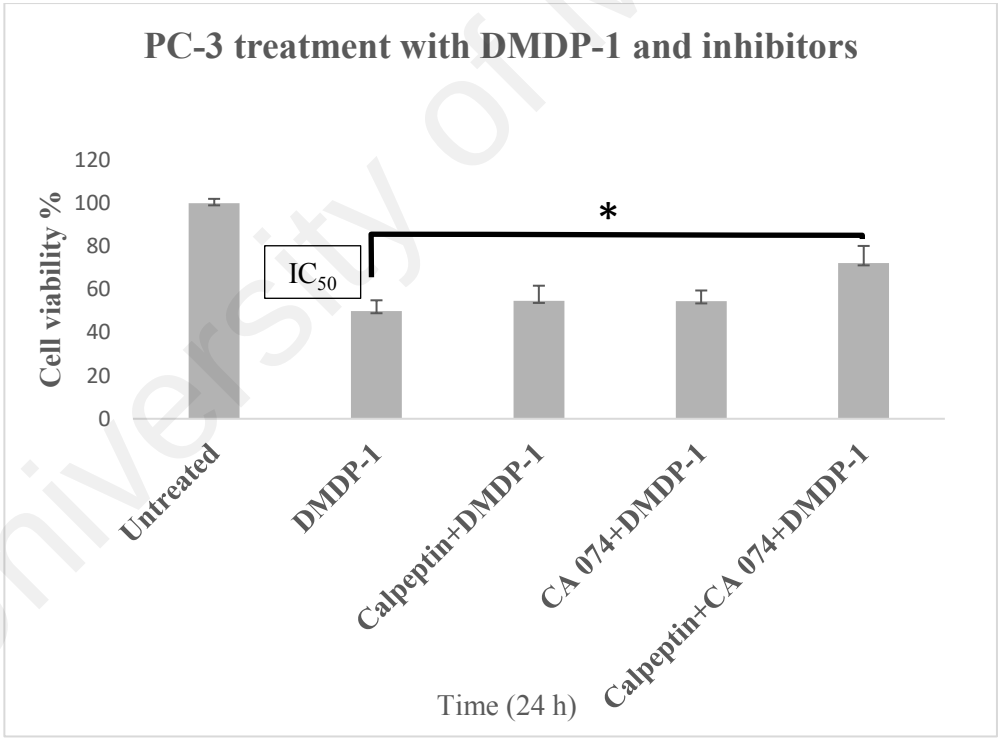


**Figure 4.9:** Roles of calpain-2 and cathepsin B in the CI-PCD induced in PC-3 and DU 145 cells. Comparative analysis with MTT assay to investigate the role of calpain-2 and cathepsin B in the cell death induction in PC-3 (A) and DU 145 (B) cells. Calpeptin and CA 074 were used to chemically inhibit calpain-2 and cathepsin B activities, respectively. Results were presented as mean normalised intensity ± S.D. of three independent experiments and (*) denotes $p < 0.05$.

B

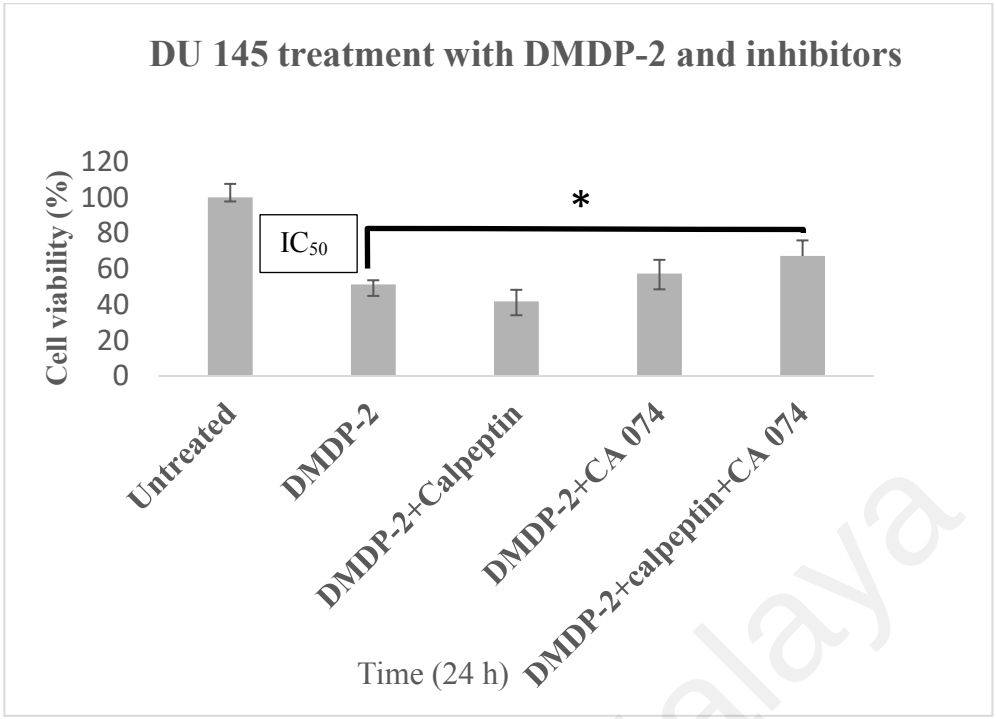


**Figure 4.9,** continued.

To further investigate the roles of calpain-2 and cathepsin B during treatment with DMDP-1 & -2, their activities were inhibited, and cell viability was assessed using the MTT assay. Calpain-2 activity was inhibited with calpeptin while cathepsin B activity was inhibited with CA-074. In both cell lines, cell death attenuation was observed when calpain-2 and cathepsin B were inhibited upon 24 h of treatment in PC-3 at 72.1% viability (Figure 4.9 A) and DU 145 at 67.2%, compared to the uninhibited control (Figure 4.9 B).

# CHAPTER 5: DISCUSSION

Natural compounds have been recognised to induce various types of PCD in cancer cells (Wang et al., 2018). Since many cancer cells bear the loss of function of the p53 tumour suppressor gene and are resistant to classical PCD such as CD-PCD (Pietsch et al., 2008), it is desirable to develop natural compounds as cancer therapeutic agents to induce alternative types of cell death. A well-known example of anti-cancer drug derived from natural compound is paclitaxel, marketed under the brand name Taxol and derived from the bark of Pacific yew, *Taxus brevifolia*. Its mechanism is mainly by inhibiting the mitotic process in cancer cells by binding to the tubulin and preventing cell division (Horwitz, 1994). However, Taxol has also been reported to induce CI-PCD in non-small lung cancer cells (NSCLC) (Huisman et al., 2002), highlighting natural compounds effectiveness against cancer cells through multiple death mechanisms.

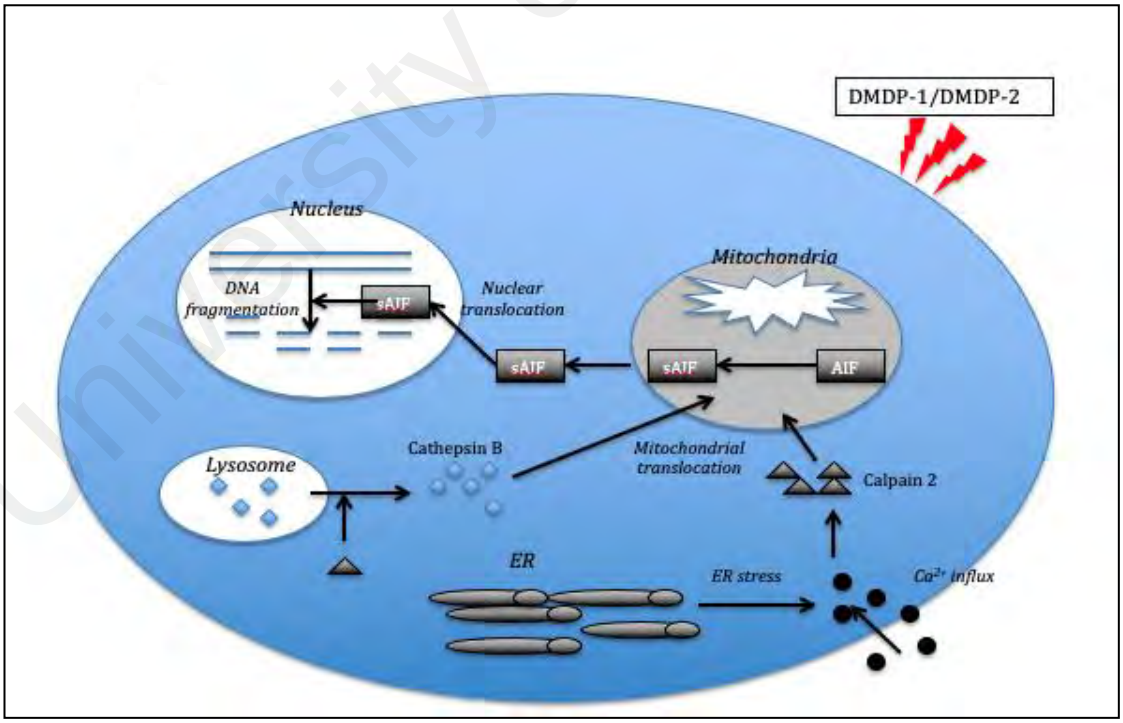


**Figure 5.1:** Hypothetical pathway of DMDP-1 & -2 mode of actions. A hypothetical pathway describing the mechanisms of CI-PCD induced by DMDP-1 & -2 in PC-3 and DU 145 cells respectively.

As a continuation from a preliminary study, the objective of this research project is to investigate the mode of action of two natural coumarin analogues, DMDP-1 and DMDP-2, that were identified to induce CI-PCD in two prostate cancer cell lines, PC-3 and DU 145 (Suparji et al., 2016). Therefore, a hypothetical pathway was proposed as the CI-PCD mechanism induced by DMDP-1 & -2 (Figure 5.1), the cells are hypothesised to undergo disruption in homeostasis balance as the initial reaction following treatment with the analogues. Next, death proteases, namely calpain-2, cathepsin B and AIF are activated to induce DNA damage as the final hallmark of cell death.

## 5.1 Disruption in cellular homeostasis

Disruption of cellular homeostasis is one of the hallmarks of cell death. The change in the cellular balance can be measured by looking into two homeostasis parameters, which are the intracellular $Ca^{2+}$ and the ER stress levels. Treatments with DMDP-1 and DMDP-2 in the prostate cancer cell lines PC-3 and DU 145 increased the intracellular $Ca^{2+}$ and the ER stress levels.

ER is an organelle in the cells that is responsible for protein translocation, folding and post-translation modification. In addition, the ER also functions as $Ca^{2+}$ storage in non-muscle cells. ER membranes contain many $Ca^{2+}$ binding proteins and related channels regulating the balance and movement of $Ca^{2+}$ in the cells (Biagioli et al., 2008; Oslowski, 2011; Krebs & Michalak, 2014).

As previously established, disturbance in the cellular-environment balance by pathological or physiological insults will lead to an accumulation of misfolded and unfolded proteins in ER lumen and eventually ER stress. This stressful condition causes an overflow of $Ca^{2+}$ into the cytoplasm to disrupt the ER functions. $Ca^{2+}$ is vital in many cellular physiological functions and highly associated with not only the homeostasis of the cell but also with the organelles. Therefore, any distortion, overload or imbalance of

$Ca^{2+}$ may lead to toxicity in cells (Orrenius et al., 2011). However, there is an undergoing debate as to whether imbalance of $Ca^{2+}$ cause ER stress in the cells or vice versa (Krebs & Michalak, 2014). Additionally, evidence from various data have reported that both ER stress and $Ca^{2+}$ accumulation in the cells often occur at a proximal time to each other (Biagioli et al., 2008; Oslowski, 2011; Torres et al., 2011). In both prostate cancer cell lines used in this study, $Ca^{2+}$ level showed a significant increase that can be interpreted as $Ca^{2+}$ overload and ER stress increase after treatment with their respective analogues. Therefore, DMDP-1 & -2 were able to induce disruption in the $Ca^{2+}$ balance and eventually trigger ER stress in the cells.

## 5.2 Activation of death proteases

### 5.2.1 Calpain-2

Calpain-2 is a cytoplasmic cysteine protease that is activated by micromolar concentration of intracellular $Ca^{2+}$. Activated calpain-2 will be auto-degraded before carrying out proteolysis of its substrates (Goll et al., 2003). Calpain-2 regulates many cellular physiological functions such as signal transduction, cytoskeletal organization, cell death and cell cycle by cleaving substrates involved in these processes (Ono et al., 2004)

Calpain-2 has also been implicated to cause cell function impairment in many pathologies such as Alzheimer's disease, type-2 diabetes and ischemia (Galvez et al., 2007; Huang et al., 2010). Although it plays a role in CD-PCD by activating caspases, it has also been reported to induce CI-PCD in neuron cells and photoreceptor of mouse retina in retinitis pigmentosa model through specific signalling pathways (Bravo-Sagua et al., 2013; Wang et al., 2018). While the actual mechanism of calpain-2 induced CI-PCD has not yet been entirely elucidated, these reports have provided evidence that calpain-2 can regulate cell death via multiple pathways.

In our study, activation of calpain-2 was detected parallel to the increase in $Ca^{2+}$ and ER stress levels that occurred immediately after treatment with the analogues. Thus, it is evident that ER stress levels and $Ca^{2+}$ overload in the cells have provided a favoured environment for calpain-2 activation (Lopatniuk & Witkowski, 2011).

### 5.2.2 Cathepsin B

Apart from calpain-2, cathepsin B, a lysosome protease is also sensitive to changes in intracellular $Ca^{2+}$. Increase in $Ca^{2+}$ levels lead to lysosomal membrane permeabilisation (LMP) to cause the release of cathepsin B into the cytosol. The switch from an acidic environment in the lysosome to a neutral pH in the cytoplasm allows the molecular modification of cathepsin B's structure and the opening of the active sites responsible for its endopeptidase activity.

Similar to calpain-2, cathepsin B has multiple roles in cell physiological functions including PCD. Cathepsin B has been reported to induce both CD-PCD and CI-PCD through various mechanisms in NSCLC exposed to micro-stabilizing agents and cervical cancer cells (HeLa) treated with doxorubicin.

Thymoquinone, another extensively studied natural compound, was reported to induce CI-PCD in glioblastoma cells mediated by cathepsin B (Racoma et al., 2013). Besides, berberine, a plant-derived isoquinoline alkaloid, was also reported to induce CI-PCD in colon cancer cell lines mediated by cathepsin B (Wang et al., 2012).

In this study, PC-3 cells treated with DMDP-1 showed a significant difference in the cathepsin B activity, but insignificantly in DMDP-2 treated DU 145 cells as a result of high basal cathepsin B activity. It has been reported that among three prostate cancer cell lines, PC-3, DU 145 and LNCaP, DU 145 possesses the highest baseline level of cathepsin

B (Podgorski et al., 2005), which validates the high cathepsin B activity in DU 145 cells in this study.

### 5.2.3 Calpain-2 and cathepsin B axis

Since calpain-2 and cathepsin B are both known to induce CD-PCD and CI-PCD, these proteases are potential targets for drug development in cancer therapy. Recently, calpain-2 and cathepsin B were shown to work together to mediate cell death in an event described as calpain-2 and cathepsin B axis. The study on a Creutzfeldt-Jakob disease has shown that an altered $Ca^{2+}$ level in the cells was able to induce cell death through the two proteases axis (Llorens et al., 2017).

These reports support the observation made in this study (Figure 4.9) in which significant attenuations of cell death were observed in DMDP-1 treated PC-3 and DMDP-2 treated DU 145 only when both calpain-2 and cathepsin were inhibited.

## 5.3 Mitochondrial membrane permeability and apoptotic inducing factor (AIF)

Besides ER, mitochondrion is another organelle in the cell that requires $Ca^{2+}$ in the signalling pathways, especially in the mitochondrial membrane transport and permeability (Orrenius et al., 2011). Transportation of proteins and ions across the mitochondrial membrane is typically regulated by various mechanisms through different protein transports or carriers. Mitochondrial permeability transition (MPT) is one of the mechanisms in mitochondrial transport that is highly regulated by the $Ca^{2+}$ and oxidative stress levels in the cells. Exposure to high levels of both $Ca^{2+}$ and oxidative stress will trigger the formation of mitochondrial pores and allow the permeabilisation of proteins of sizes up to 1500 Dalton. Moreover, high MPT will eventually increase the $\Delta\psi M$ and lead to mitochondrial membrane depolarisation, which will allow an uninhibited flow of ions and certain proteins across the membrane (Schinder et al., 1996; White & Reynolds, 1996). The charge imbalance that results from the generation of an electrochemical

gradient across the MIM forms the basis of the ΔψM. The significant change in ΔψM observed in the cells upon treatment with DMDP-1 & -2 indicated a disruption of the membrane integrity and release of AIF from the MIM into the cytoplasm.

AIF is one of the first discovered proteases with the ability to induce CI-PCD not only in tumour cells but also in injury and neurodegenerative diseases (Cregan et al., 2004; Constantinou et al., 2009). Truncated AIF (57kDa) from the mitochondria conventionally will be released to the cytoplasm and further translocated into the nucleus to induce large DNA fragmentation (Constantinou et al., 2009). However, in this study, no AIF was observed in the nucleus following the release to the cytoplasm. This is in accordance with the previous study where there was no DNA laddering observed in the cells upon treatment.

### 5.4 Reactive oxygen species (ROS) formation and DNA damage by ROS

DNA damage is an important parameter that characterises PCD. The absence of DNA laddering in the previous study (Suparji et al., 2016) has directed this study to examine other possible DNA damage mechanism. PCD is usually accompanied by shift of the redox balance, as well as increase in free radicals such as superoxide anion, lipid peroxidation and oxidative damage of membranes and DNA. Besides, the mitochondrial protein analysis demonstrated the release of truncated-mature AIF to the mitochondria, which suggested involvement of AIF in the production of ROS in the cells. Mature AIF purifies as a flavoprotein that carries an electron transfer (redox) function. AIF belongs to the electron-transferase class of NADH reductases, due to its rapid reaction to oxygen to form superoxide ($O_2^-$) and the flavoprotein neutral radical as products (Miramar et al., 2001).

As expected, upon treatment, increased level of ROS-superoxide ($O_2^-$) was observed, which induced toxicity through oxidative stress (Han & Chen, 2013). The increase in the superoxide level observed in this study showed that DMDP-1 &-2 were able to induce oxidative stress in the prostate cancer cells.

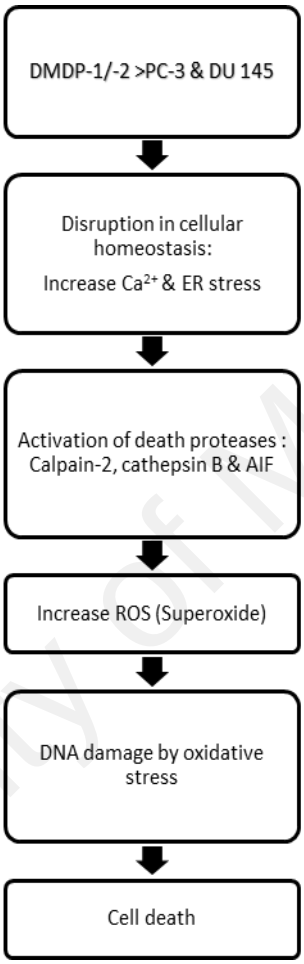


**Figure 5.2:** Theoretical pathway of DMDP-1 & -2 mode of actions in PC-3 and DU 145 cell lines. A summary of CI-PCD induced by DMDP-1 & -2 in PC-3 and DU 145 cells respectively.

Oxidative stress is resulted from the imbalance manifestation and overproduction of ROS. The free radical of ROS, superoxide, is a threat to the cells and DNA as the free radicals from any species of ROS are able to disrupt the DNA chemical bonds.

A by-product of oxidative DNA damage, 8-hydroxy-2'-deoxyguanosine (8-OHdG), is a biomarker used to evaluate DNA damage caused by endogenous oxidative stress (Barzilai & Yamamoto, 2004; Tabak et al., 2011). The 8-OHdG level is known to be higher in cancer including prostate cancer cells (Barzilai & Yamamoto, 2004), treatments with the analogues were proven to significantly increase the 8-OHdG level in PC-3 and DU 145 cells.

In conclusion, natural compound analogues DMDP-1 & -2 induce CI-PCD in prostate cancer cell lines PC-3 and DU 145 by disrupting the cellular homeostasis, activating death proteases calpain-2, cathepsin B and AIF, and increasing ROS formation, which finally lead to DNA damage caused by oxidative stress (Figure 5.2).

# CHAPTER 6: CONCLUSION

The potentials of natural compounds as therapeutic agents for cancer treatments through various pathways is very well established. As indicated in the subjects of this study, geranylated 4-phenylcoumarin DMDP-1 & -2 were shown to be able to induce programmed cell death in the prostate cancer cell lines independent of caspases (CI-PCD).

The observation of all the cell death parameters where shown to be affected by the treatment. First, the analogues were able to disrupt the prostate cancer cells cellular homeostasis as observed in the elevation of both $Ca^{2+}$ levels and the ER stress levels.

Multiple death proteases which were calpain-2, cathepsin B and AIF were also shown to be vital in the in the induction of the CI-PCD. The cytoplasmic death proteases calpain-2 and cathepsin B activities were shown to increase in DMDP-1 treated PC-3 cells lines, and calpain2 in DMDP-2 treated DU 145 cells. Interestingly, even there's no significant increase in DU 145 cells' cathepsin activity observed after treatment, attenuation of cell death in both cell lines were observed only when both calpain-2 and cathepsin B were inhibited. Which means that, these two proteases synergistically induce CI-PCD in the prostate cancer cells.

The mitochondrion was also shown to have a role in the CI-PCD induced by the analogues. Reduction of mitochondrial membrane potential was observed indicating there was interruption in the cells mitochondrial balance. Feasibly, the mitochondrial death protease AIF was also shown to be released into the cytoplasm.

Finally, the analogues were able to increase the ROS levels which lead to the DNA damage in both prostate cancer cell lines.

This study has provided an understanding on the analogues against two androgen-independent prostate cancer cell lines. Geranylated 4-phenylcoumarins are capable to induce caspase-independent programmed cell death in prostate cancer cell lines in a systematic manner and therefore, are potentially important anti-cancer agents worth to be further studied.

## REFERENCES


Ameisen, J. C. (2002). On the origin, evolution, and nature of programmed cell death: A timeline of four billion years. *Cell Death and Differentiation, 9*(4), 367-393.

Appelqvist, H., Johansson, A. C., Linderoth, E., Johansson, U., Antonsson, B., Steinfeld, R., . . . Ollinger, K. (2012). Lysosome-mediated apoptosis is associated with cathepsin D-specific processing of bid at Phe24, Trp48, and Phe183. *Annals of Clinical & Laboratory Science, 42*(3), 231-242.

Barzilai, A., & Yamamoto, K. (2004). DNA damage responses to oxidative stress. *DNA Repair, 3*(8-9), 1109-1115.

Biagioli, M., Pifferi, S., Ragghianti, M., Bucci, S., Rizzuto, R., & Pinton, P. (2008). Endoplasmic reticulum stress and alteration in calcium homeostasis are involved in cadmium-induced apoptosis. *Cell Calcium, 43*(2), 184-195.

Boya, P., & Kroemer, G. (2008). Lysosomal membrane permeabilization in cell death. *Oncogene, 27*(50), 6434-6451.

Brand, M. D., Orr, A. L., Perevoshchikova, I. V., & Quinlan, C. L. (2013). The role of mitochondrial function and cellular bioenergetics in ageing and disease. *British Journal of Dermatology, 169 Suppl 2*, 1-8.

Bravo-Sagua, R., Rodriguez, A. E., Kuzmicic, J., Gutierrez, T., Lopez-Crisosto, C., Quiroga, C., . . . Lavandero, S. (2013). Cell death and survival through the endoplasmic reticulum-mitochondrial axis. *Current Molecular Medicine, 13*(2), 317-329.

Bray, F., Ferlay, J., Soerjomataram, I., Siegel, R. L., Torre, L. A., & Jemal, A. (2018). Global cancer statistics 2018: GLOBOCAN estimates of incidence and mortality worldwide for 36 cancers in 185 countries. *A Cancer Journal for Clinicians, 68*(6), 394-424.

Broker, L. E., Kruyt, F. A., & Giaccone, G. (2005). Cell death independent of caspases: a review. *Clinical Cancer Research, 11*(9), 3155-3162.

Caldwell, G. W., Yan, Z., Lang, W., & Masucci, J. A. (2012). The IC(50) concept revisited. *Curr Top Med Chem, 12*(11), 1282-1290.

Cerella, C., Diederich, M., & Ghibelli, L. (2010). The dual role of calcium as messenger and stressor in cell damage, death, and survival. *International Journal of Cell Biology 2010*, Article#546163.

Charras, G. T. (2008). A short history of blebbing. *Journal of Microscopy, 231*(3), 466-478.

Constantinou, C., Papas, K. A., & Constantinou, A. I. (2009). Caspase-independent pathways of programmed cell death: the unraveling of new targets of cancer therapy? *Current Cancer Drug Targets, 9*(6), 717-728.

Cooper, G.M. (2000). The development and causes of cancer. *In The Cell: A Molecular Approach* (2nd ed.) Suncerland (MA): Sinauer Associates

Cregan, S. P., Dawson, V. L., & Slack, R. S. (2004). Role of AIF in caspase-dependent and caspase-independent cell death. *Oncogene, 23*, 2785.

Elmore, S. (2007). Apoptosis: a review of programmed cell death. *Toxicologic Pathology, 35*(4), 495-516.

Fitzwalter, B. E., & Thorburn, A. (2015). Recent insights into cell death and autophagy. *The FEBS Journal, 282*(22), 4279-4288.

Galvez, A. S., Diwan, A., Odley, A. M., Hahn, H. S., Osinska, H., Melendez, J. G., . . . Dorn, G. W., 2nd. (2007). Cardiomyocyte degeneration with calpain deficiency reveals a critical role in protein homeostasis. *Circulation Research, 100*(7), 1071-1078.

Garcia-Ayllon, M. S., Small, D. H., Avila, J., & Saez-Valero, J. (2011). Revisiting the role of acetylcholinesterase in Alzheimer's disease: Cross-talk with p-tau and beta-amyloid. *Frontiers of Molecular Neurosciences, 4*, 22.

Goll, D. E., Thompson, V. F., Li, H., Wei, W., & Cong, J. (2003). The calpain system. *Physiological Reviews, 83*(3), 731-801.

Gomathi, C. (2015) Bioactive 4-phenylcoumarins from *Mesua elegans* and *Mesua kunstleri* (Doctoral dissetrtation, University of Malaya, Kuala Lumpur, Malaysia). Retrieved from http://studentsrepo.um.edu.my/6521/1/Chan_Gomathi_PhD_ Thesis.pdf

Han, Y., & Chen, J. Z. (2013). Oxidative stress induces mitochondrial DNA damage and cytotoxicity through independent mechanisms in human cancer cells. *BioMed Research International, 2013*, 825065.

Hirsch, T., Marchetti, P., Susin, S. A., Dallaporta, B., Zamzami, N., Marzo, I., . . . Kroemer, G. (1997). The apoptosis-necrosis paradox. Apoptogenic proteases activated after mitochondrial permeability transition determine the mode of cell death. *Oncogene, 15*(13), 1573-1581.

Horwitz, S. B. (1994). Taxol (paclitaxel): Mechanisms of action. *Annals of Oncology, 5 Suppl 6*, S3-6.

Hoult, J. R., & Paya, M. (1996). Pharmacological and biochemical actions of simple coumarins: natural products with therapeutic potential. *General Pharmacology, 27*(4), 713-722.

Huang, C. J., Gurlo, T., Haataja, L., Costes, S., Daval, M., Ryazantsev, S., . . . Butler, P. C. (2010). Calcium-activated calpain-2 is a mediator of beta cell dysfunction and apoptosis in type 2 diabetes. *Journal of Biological Chemistry, 285*(1), 339-348.

Huisman, C., Ferreira, C. G., Broker, L. E., Rodriguez, J. A., Smit, E. F., Postmus, P. E., . . . Giaccone, G. (2002). Paclitaxel triggers cell death primarily via caspase-independent routes in the non-small cell lung cancer cell line NCI-H460. *Clinical Cancer Research, 8*(2), 596-606.

Kerr, J. F., Wyllie, A. H., & Currie, A. R. (1972). Apoptosis: A basic biological phenomenon with wide-ranging implications in tissue kinetics. *British Journal of Cancer, 26*(4), 239-257.

Kochummen, K. M. (1998). *Mesua elegans*.The IUCN Red List of Threatened Species. Retrieved from https://www.iucnredlist.org/species/31837/9664099

Kostova, I. (2006). Synthetic and natural coumarins as antioxidants. *Mini-Reviews in Medicinal Chemistry, 6*(4), 365-374.

Kourtis, N., & Tavernarakis, N. (2009). Autophagy and cell death in model organisms. *Cell Death and Differentiation, 16*(1), 21-30.

Krebs J, A. L., Michalak M. (2014). Ca(2+) homeostasis and endoplasmic reticulum (ER) stress: An integrated view of calcium signaling. *Biochemical and Biophysical Research Communications, 460*(1), 114-121.

Kroemer, G., Galluzzi, L., & Brenner, C. (2007). Mitochondrial membrane permeabilization in cell death. *Physiological Reviews 87*(1), 99-163.

Kumari, S., Badana, A. K., G, M. M., G, S., & Malla, R. (2018). Reactive oxygen species: A key constituent in cancer survival. *Biomarker Insights, 13*, 1177271918755391.

Lakhtakia, R. (2014). A brief history of breast cancer: Part I: Surgical domination reinvented. *Sultan Qaboos University Medical Journal, 14*(2), e166-169.

Liou, G. Y., & Storz, P. (2010). Reactive oxygen species in cancer. *Free Radical Research, 44*(5), 479-496.

Llorens, F., Thune, K., Sikorska, B., Schmitz, M., Tahir, W., Fernandez-Borges, N., . . . Zerr, I. (2017). Altered Ca(2+) homeostasis induces Calpain-Cathepsin axis activation in sporadic Creutzfeldt-Jakob disease. *Acta Neuropathologica Communications, 5*(1), 35.

Lopatniuk, P., & Witkowski, J. M. (2011). Conventional calpains and programmed cell death. *Acta Biochimica Polonica, 58*(3), 287-296.

Loreto, C., La Rocca, G., Anzalone, R., Caltabiano, R., Vespasiani, G., Castorina, S., . . . Sansalone, S. (2014). The role of intrinsic pathway in apoptosis activation and progression in Peyronie's disease. *BioMed Research International, 2014*, Article#616149.

McDonnell, T. J., Troncoso, P., Brisbay, S. M., Logothetis, C., Chung, L. W., Hsieh, J. T., . . . Campbell, M. L. (1992). Expression of the protooncogene bcl-2 in the prostate and its association with emergence of androgen-independent prostate cancer. *Cancer Research, 52*(24), 6940-6944.

McIlwain, D. R., Berger, T., & Mak, T. W. (2013). Caspase functions in cell death and disease. *Cold Spring Harbor Perspectives in Biology, 5*(4), Article#a008656.

Miramar, M. D., Costantini, P., Ravagnan, L., Saraiva, L. M., Haouzi, D., Brothers, G., . . . Susin, S. A. (2001). NADH oxidase activity of mitochondrial apoptosis-inducing factor. *Journal of Biological Chemistry, 276*(19), 16391-16398.

Murray, A. P., Faraoni, M. B., Castro, M. J., Alza, N. P., & Cavallaro, V. (2013). Natural AChE Inhibitors from Plants and their Contribution to Alzheimer's Disease Therapy. *Current Neuropharmacology, 11*(4), 388-413.

Nelson, J. B., & Carducci, M. A. (2000). The role of endothelin-1 and endothelin receptor antagonists in prostate cancer. *BJU International, 85 Suppl 2*, 45-48.

Nobili, S., Lippi, D., Witort, E., Donnini, M., Bausi, L., Mini, E., & Capaccioli, S. (2009). Natural compounds for cancer treatment and prevention. *Pharmacol Res, 59*(6), 365-378.

Ohta, S., Yanagihara, K., & Nagata, K. (1997). Mechanism of apoptotic cell death of human gastric carcinoma cells mediated by transforming growth factor beta. *Biochemical Journal, 324 (3)*, 777-782.

Ono, Y., Kakinuma, K., Torii, F., Irie, A., Nakagawa, K., Labeit, S., . . . Sorimachi, H. (2004). Possible regulation of the conventional calpain system by skeletal muscle-specific calpain, p94/calpain 3. *Journal of Biological Chemistry, 279*(4), 2761-2771.

Orrenius, S., Nicotera, P., & Zhivotovsky, B. (2011). Cell death mechanisms and their implications in toxicology. *Toxicological Sciences, 119*(1), 3-19.

Oslowski CM, U. F. (2011). Measuring ER stress and the unfolded protein response using mammalian tissue culture system. *Methods in Enzymology, 490*, 71-92.

Phaniendra, A., Jestadi, D. B., & Periyasamy, L. (2015). Free radicals: Properties, sources, targets, and their implication in various diseases. *Indian Journal of Clinical Biochemistry, 30*(1), 11-26.

Pietsch, E. C., Sykes, S. M., McMahon, S. B., & Murphy, M. E. (2008). The p53 family and programmed cell death. *Oncogene, 27*(50), 6507-6521.

Podgorski, I., Linebaugh, B. E., Sameni, M., Jedeszko, C., Bhagat, S., Cher, M. L., & Sloane, B. F. (2005). Bone microenvironment modulates expression and activity of cathepsin B in prostate cancer. *Neoplasia, 7*(3), 207-223.

Qi, R., & Liu, X. Y. (2006). New advance in caspase-independent programmed cell death and its potential in cancer therapy. *Internatiol Journal of Biomedical Sciences, 2*(3), 211-216.

Racoma, I. O., Meisen, W. H., Wang, Q.-E., Kaur, B., & Wani, A. A. (2013). Thymoquinone inhibits autophagy and induces cathepsin-mediated, caspase-independent cell death in glioblastoma cells. *PLos One, 8*(9), Article#e72882.

Rager, J.E. (2015). Chapter 8 - The role of apoptosis-associated pathways as responders to contaminants and in disease progression. *Systems Biology in Toxicology and Environmental Health*, 187-205.

Repnik, U., Cesen, M. H., & Turk, B. (2013). The endolysosomal system in cell death and survival. *Cold Spring Harbour Perspectives in Biology, 5*(1), Article#a008755.

Repnik, U., Hafner Cesen, M., & Turk, B. (2014). Lysosomal membrane permeabilization in cell death: Concepts and challenges. *Mitochondrion, Volume 19 Partt A*, 49-57.

Salmon, T. B., Evert, B. A., Song, B., & Doetsch, P. W. (2004). Biological consequences of oxidative stress-induced DNA damage in *Saccharomyces cerevisiae. Nucleic Acids Research, 32*(12), 3712-3723.

Sano, R., & Reed, J. C. (2013). ER stress-induced cell death mechanisms. *Biochimica et Biophysica Acta, 1833*(12), 3460-3470.

Sarin, A., Williams, M. S., Alexander-Miller, M. A., Berzofsky, J. A., Zacharchuk, C. M., & Henkart, P. A. (1997). Target cell lysis by CTL granule exocytosis is independent of ICE/Ced-3 family proteases. *Immunity, 6*(2), 209-215.

Schulz, W. A., Burchardt, M., & Cronauer, M. V. (2003). Molecular biology of prostate cancer. *Molecular Human Reproduction, 9*(8), 437-448.

Schinder, A. F., Olson, E. C., Spitzer, N. C., & Montal, M. (1996). Mitochondrial dysfunction is a primary event in glutamate neurotoxicity. *The Journal of Neuroscience, 16*(19), 6125-6133.

Smith, M. A., & Schnellmann, R. G. (2012). Calpains, mitochondria, and apoptosis. *Cardiovascular Research, 96*(1), 32-37.

Sothilingam, S., Sundram, M., Malek, R., & Sahabuddin, R. M. (2010). Prostate cancer screening perspective, Malaysia. *Urologic Oncology, 28*(6), 670-672.

Srinivas, U. S., Tan, B. W. Q., Vellayappan, B. A., & Jeyasekharan, A. D. (2018). ROS and the DNA damage response in cancer. *Redox Biology*, Article#101084.

Suparji NS, C. G., Sapili H, Arshad NM, In LLA, Awang K, Nagoor NH. (2016). Geranylated 4-phenylcoumarins exhibit anticancer effects against human prostate cancer cells through caspase-independent mechanism. *PLos One, 11*(3), Article#4790937.

Surova, O., & Zhivotovsky, B. (2013). Various modes of cell death induced by DNA damage. *Oncogene, 32*(33), 3789-3797.

Suzuki, K., Bose, P., Leong-Quong, R. Y. Y., Fujita, D. J., & Riabowol, K. (2010). REAP: A two-minute cell fractionation method. *BMC Research Notes, 3*(1), 294.

Tabak, O., Gelisgen, R., Erman, H., Erdenen, F., Muderrisoglu, C., Aral, H., & Uzun, H. (2011). Oxidative lipid, protein, and DNA damage as oxidative stress markers in vascular complications of diabetes mellitus. *Clinical and Investigative Medicine, 34*(3), 163-171.

Tait, S. W., & Green, D. R. (2008). Caspase-independent cell death: Leaving the set without the final cut. *Oncogene, 27*(50), 6452-6461.

Tosun, A. (2012). *Biotechnological production of plant secondary metabolites*: Bentham Science

Torres, M., Encina, G., Soto, C., & Hetz, C. (2011). Abnormal calcium homeostasis and protein folding stress at the ER: A common factor in familial and infectious prion disorders. *Communicative Integrative Biology, 4*(3), 258-261.

Tung, N. H., Uto, T., Sakamoto, A., Hayashida, Y., Hidaka, Y., Morinaga, O., . . . Shoyama, Y. (2013). Antiproliferative and apoptotic effects of compounds from the flower of *Mammea siamensis* (Miq.) T. Anders. on human cancer cell lines. *Bioorganic and Medicinal Chemistry Letters, 23*(1), 158-162.

Volbracht, C., Chua, B. T., Ng, C. P., Bahr, B. A., Hong, W., & Li, P. (2005). The critical role of calpain versus caspase activation in excitotoxic injury induced by nitric oxide. *Journal of Neurochemistry, 93*(5), 1280-1292.

Wang, Y., Zhong, J., Bai, J., Tong, R., An, F., Jiao, P., . . . Cai, L. (2018). The Application of Natural Products in Cancer Therapy by Targeting Apoptosis Pathways. *Current Drug Metabolism, 19*(9), 739-749.

White, R. J., & Reynolds, I. J. (1996). Mitochondrial depolarization in glutamate-stimulated neurons: An early signal specific to excitotoxin exposure. *The Journal of Neuroscience, 16*(18), 5688-5697.

WHO, World Health Organization (2018, September 12). Cancer. Retrieved from http://www.who.int/news-room/fact-sheets/detail/cancer

Yang, H., Villani, R. M., Wang, H., Simpson, M. J., Roberts, M. S., Tang, M., & Liang, X. (2018). The role of cellular reactive oxygen species in cancer chemotherapy. *Journal of Experimental and Clinical Cancer Research, 37*(1), 266.

Zhivotovsky, B., & Orrenius, S. (2010a). Cell cycle and cell death in disease: Past, present and future. *Journal of Internal Medicine, 268*(5), 395-409. doi:10.1111/j.1365-2796.2010.02282.x

Zhivotovsky, B., & Orrenius, S. (2010b). Cell death mechanisms: Cross-talk and role in disease. *Experimental Cell Research, 316*(8), 1374-1383.

Ziegler, U., & Groscurth, P. (2004). Morphological features of cell death. *News in Physiological Sciences, 19*, 124-128.

## LIST OF PUBLICATIONS AND PAPERS PRESENTED

### PAPERS PRESENTED

1. **Hani, S.,** & Nagoor, N.H. (2019). *Elucidation of Calpain-2 and Cathepsin B involvement in caspase-independent programmed cell death induced by 4-phenylcoumarins isolated from Mesua elegans in prostate cancer cell line*. Paper presented at 3rd International Conference for Molecular Biology & Biotechnology (ICMBB), 24th – 25th April 2019, Kuala Lumpur, Malaysia.

2. **Hani, S.,** & Nagoor, N. H. (2019). *Characterization of caspase-independent programmed cell death mechanism induced by geranylated 4-phenylcoumarins in prostate cancer cell lines.* Paper presented at Nara Institute of Science and Technology (NAIST) Pre-screening Internship, 15th – 24th January 2019, Nara Institute of Science and Technology, Nara, Japan.

3. **Hani, S.,** & Nagoor, N. H. (2017). *Elucidation of Calpain-2 and Cathepsin B involvement in caspase-independent programmed cell death induced by 4-phenylcoumarins isolated from Mesua elegans in prostate cancer cell line*. Poster presentation. 2nd International Conference for Molecular Biology & Biotechnology (ICMBB), 1st – 2nd November 2017, Kuala Lumpur, Malaysia